Russian Chemical Reviews **72** (12) 1011 – 1034 (2003) © 2003 Russian Academy of Sciences and Turpion Ltd

DOI 10.1070/RC2003v072n12ABEH000796

X-Ray spectra and electronic structure of boron compounds †

V D Yumatov, E A Il'inchik, V V Volkov

Contents

I.	Introduction	1011
II.	Characteristics of boron compounds, their structures and chemical bonds	1011
III.	The physical bases of X-ray spectroscopy	1016
IV.	X-Ray spectroscopy and electronic structure of boron compounds	1019
V.	Conclusion	1031

Abstract. The state-of-the-art in boron chemistry, the characteristic features of boron compounds and crystalline phases based on them, the chemical bonds in these compounds and their electronic structures are considered. The physical principles of X-ray spectroscopy and the results it provided on the chemical structures of boron compounds and the nature of chemical bonds in them are discussed. Data for X-ray photoelectron and ultraviolet photoelectron spectroscopies for various elemental boron modifications, boron oxide phases, borides, nitrides, halides, derivatives of boron hydrides and carboranes, as well as metalloboranes are compared. The bibliography includes 247 references.

I. Introduction

The chemistry of elemental boron, its compounds and crystalline phases based on them is currently a vast and quite complicated scientific field at the boundary of inorganic and organoelement chemistry. Boron compounds are successfully used in various areas of materials science, in catalysis, inorganic and organic synthesis, biochemistry, agriculture, medicine, *etc*. The fundamental and applied aspects of boron chemistry are covered in sufficient detail in numerous papers, reviews and monographs and in patent literature. The publication of a festschrift on boron chemistry and special journal issues on the subject [1–3] is evidence of the great scientific and practical value of this field of science.

The study of bond nature in compounds by both theoretical and experimental methods providing information about electronic structure is a task of current interest in modern chemistry. The results of such studies allow explanation of physicochemical properties of compounds and their reactivities and forecast ways for their synthesis. In this review, we generalise the main data of studies on the electronic structures and characteristics of chemical bonds in boron compounds by X-ray emission and X-ray absorption spectroscopies (XES and XAS, respectively). Special attention is focused on the use of these methods in combination with X-ray photoelectron spectroscopy (XPS) and ultraviolet photoelectron spectroscopy (UPS). The role of quantum-chemical calculations in interpreting the spectra is also considered. In order to systematise data from numerous publications, we first discuss the state-of-the-art of boron chemistry and specific features of chemical bonding and coordination in the most typical classes of boron compounds and then briefly present the principles and experimental fundamentals of XPS, UPS, XES and XAS. The results of X-ray spectral studies are generalised for the main classes of boron compounds; emphasis is made on those classes that have been considered in lesser detail in previous reviews, particularly, on boron hydride compounds. Finally, we discuss the relationship between the discovered features of the electronic structures of boron compounds and their physicochemical characteristics.

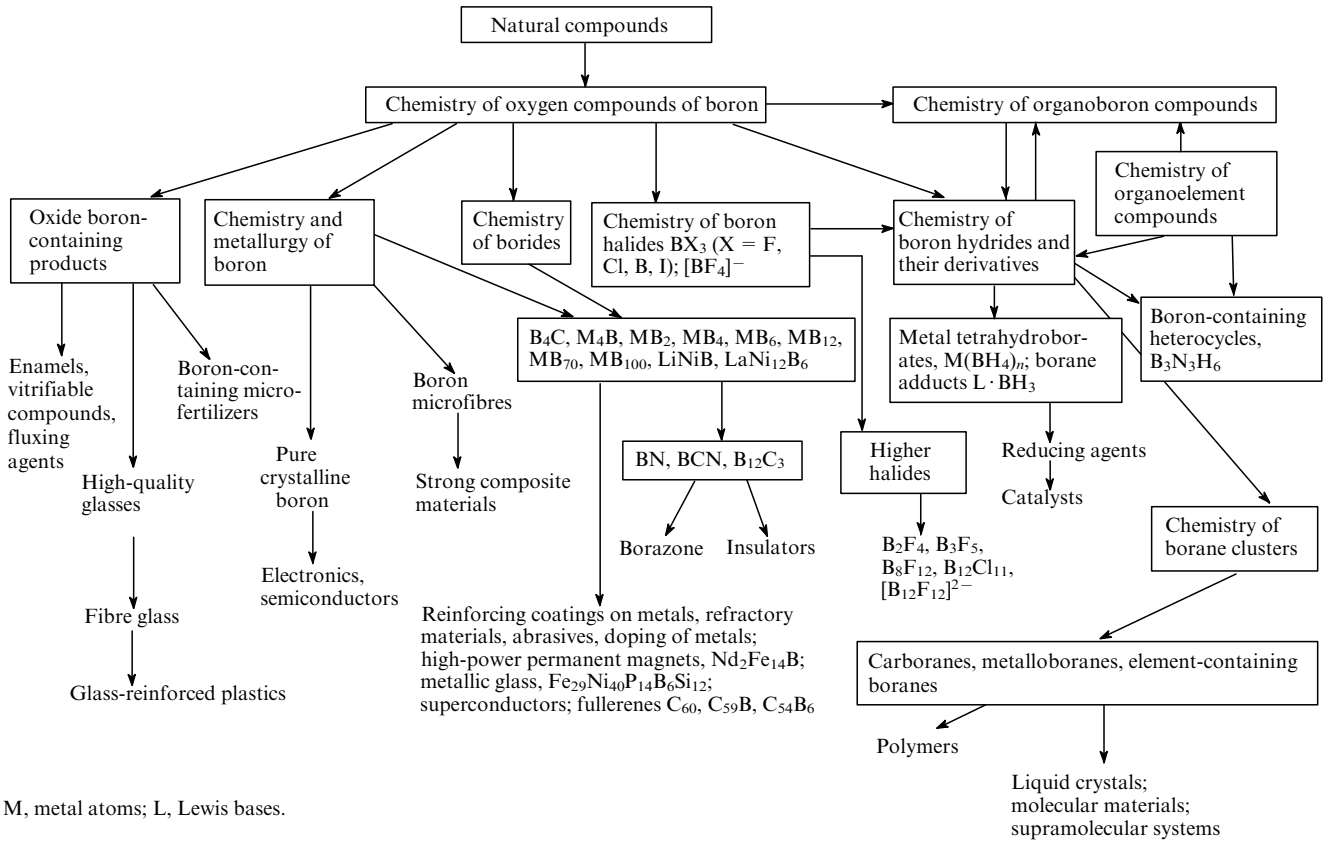
V D Yumatov, E A Il'inchik, V V Volkov A V Nikolaev Institute of Inorganic Chemistry, Siberian Branch of the Russian Academy of Sciences, Prosp. Akad. Lavrent'eva 3, 630090 Novosibirsk, Russian Federation. Fax (7-383) 234 44 89. Tel. (7-383) 234 39 75 (V V Volkov)

Received 14 November 2002
Uspekhi Khimii **72** (12) 1141 – 1166 (2003); translated by S S Veselyi

II. Characteristics of boron compounds, their structures and chemical bonds

A boron atom ($z = 5$) has the $1s^2 2s^2 2p^1$ electronic configuration. When boron or boron compounds form solid phases, the valence electrons assume a more energetically favourable configuration, *viz*., $1s^2 2s^1 2p^2$, where the boron atom has four valence atomic orbitals (AO) 2s, $2p_x$, $2p_y$, $2p_z$ and only three valence electrons.[4,5] A specific feature of this configuration is that, owing to the small covalent atomic radius of boron (0.80 – 1.01 Å) and ionic radius of B^{3+} [0.15 Å and 0.25 Å for coordination numbers (CN) 3 and 4, respectively], the electrons of a boron atom and the AOs are localised in the strong field of the nucleus with relatively weak shielding [the first ionisation potential (*IP*) of a B atom equals 8.3 eV].[6] This feature imparts unusual chemical properties to boron, which allow this element with a simple electronic structure to form a very complex system of compounds and crystalline phases characterised by numerous types of chemical bonding. In particular, it is noteworthy that a boron atom can form σ-bonds involving AOs in the sp^2 configuration, *e.g*., in such molecules as BX_3 (where X is a halogen), BR_3, *etc*. The vacant $2p_z$-AO predetermines the strong electron-acceptor properties of boron, which interacts with electron donors to give adducts and complexes of the $R_3N \cdot BH_3$, $BX_3 \cdot NH_3$, $Me_2O \cdot BF_3$, $[BF_4]^-$, and $[BPh_4]^-$ types. Multi-centred (mainly three-centred) bonds are formed in cluster-type boron hydrides and their derivatives, certain borides and elementary boron.[3–5] Such compounds refer to electron-deficient systems. These compounds contain fewer valence electrons than is required to form electron pairs between neighbouring atoms that form chemical bonds. For example, a diborane(6) molecule (B_2H_6) contains 12 valence electrons (six

† Dedicated to the 100th anniversary of Academician Anatoly Vasil'evich Nikolaev, the author of many classical works in borate chemistry.



M, metal atoms; L, Lewis bases.

Figure 1. Trends in modern boron chemistry.

pairs), which enable the formation of seven bonds: six B—H bonds and one B—B bond. The electronic structures of this type of molecule are described using the multi-centred two-electron bond concept within the molecular orbital (MO) method. Study of the electronic structures of numerous boron compounds of various types by theoretical (quantum-chemical) and experimental methods is a topical problem.

Figure 1 shows schematically the directions of modern boron chemistry. This is not a comprehensive scheme, but we will use it to determine the order for presenting and discussing experimental data. We will focus the most attention on certain reviews concerning boron chemistry and on experimental methods.

The starting materials for the preparation of boron compounds, boron-containing products and materials based on them include oxide derivatives extracted from ores (boron oxide, boric acid, borates, peroxyborates).[4,7–11] The complexity of the crystal structures of B_2O_3, various modifications of boric acid and structures of borate and polyborate anions in solutions and in crystalline phases has been noted.[4,10,11] Figure 2 shows the structures of a number of oxide boron compounds and their typical fragments. In oxygen compounds, the coordination number of a boron atom can be equal to three (sp^2-hybridisation and π-bonds) or four (sp^3-hybridisation and only σ-bonds). The lamellar structure of orthoboric acid[10] consists of triclinic cells, each containing four $B(OH)_3$ molecules, that are held by hydrogen bonds (=B—O—H···O—B=) to a considerable extent (their lengths are 2.72 Å if the boron coordination number is equal to three). Each oxygen atom is involved in hydrogen bonds with two hydrogen atoms. Studies of this system are of interest for revealing the effect of hydrogen bonds on the electronic structures of the constituent atoms. The structures of polyborate anions are more complex:[10,11] ions containing from 1 to 6 or 9 boron atoms, such as $[B_5O_7(OH)_4]^{3-}$, $\{B_9O_{14}(OH)_4[OB(OH)_2]_2\}^{7-}$, *etc.*, can be present in salts of these anions, both in solutions and in crystals. A six-membered heterocycle boroxol is the main structural fragment of polyborate anions; this can be part of monomeric,

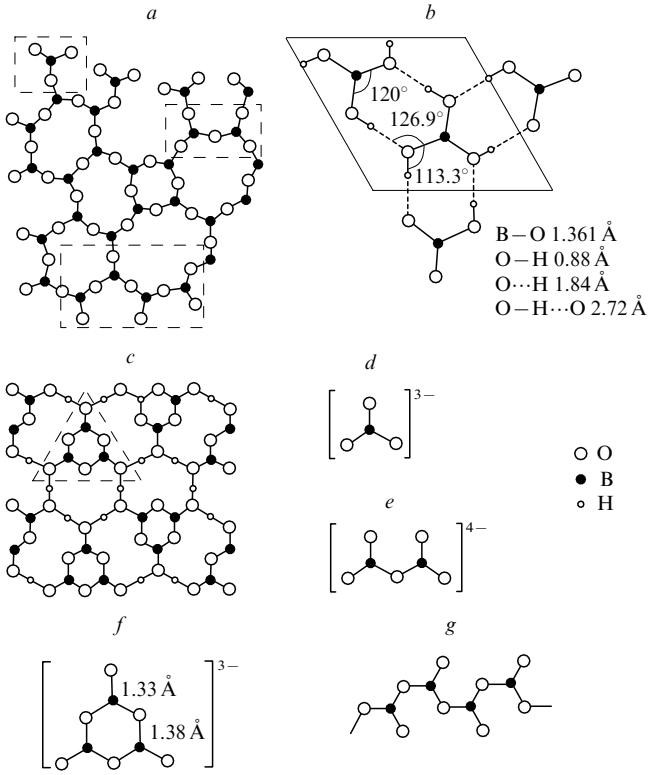


Figure 2. Fragments of structures of some oxygen-containing boron compounds.
(*a*) Glassy boric anhydride (B_2O_3);[8] (*b*) orthoboric acid $[B(OH)_3]$;[10] (*c*) lamellar structure of orthorhombic metaboric acid (HBO_2);[4,8,10] (*d*–*g*) structural fragments of borates (marked by dashed lines in Fig. 2 *a*,*c*).[4,8,10,11]

polymeric and 'fused' polycyclic structures containing oxygen atoms with CN = 3.

Numerous publications deal with the preparation of pure boron, study of its structure and properties and technological and applied aspects of its usage (see, *e.g.*, the reviews and monographs [4, 5, 8, 10, 12–14]). Elementary crystalline boron is an exceptionally 'difficult' subject. Studies of the structures of its crystalline phases and the respective physical properties are complicated by the fact that over ten polymorphic modifications of boron are known.[5, 12] The three most stable polymorphic modifications of fused boron have been characterised reliably: the α-rhombohedral (B_{12}), α-tetragonal (B_{50}) and β-rhombohedral modifications (B_{105}). Figure 3 shows fragments of certain crystal structures of boron. The β-rhombohedral form is thermodynamically most favourable.[10, 12, 14] Amorphous boron phases are also known; they are generally formed at relatively low temperatures. Difficulties in the preparation of chemically pure samples of individual boron phases are caused by its high melting point (2450 K), its considerable chemical reactivity (*i.e.*, high probability of contamination by admixtures from the gaseous environment and from the equipment) and the large number of crystal modifications with slow phase transitions between them. All these facts should be taken into consideration in studies and interpretation of the data on boron properties. An icosahedron with I_h symmetry is the structure-forming element of crystalline boron phases, 12 boron atoms with coordination numbers 5 occupy its vertices (B_{12}) (the coordination number is 6 in the formation of bonds between the B_{12} clusters), the B–B interatomic distances are equal to 1.73–1.79 Å (see Fig. 3 *a*).[2, 10] Owing to the electron deficiency and the relatively high ionisation energy of boron atoms (8.298 eV [15]), the B–B bond has substantially covalent rather than metallic character.[10] Polymorphic modifications differ in the spatial arrangements of the B_{12} icosahedra, the nature of bonds between them and the coordination numbers of boron atoms. Figure 3 *b* shows an example of the mutual arrangement of the B_{12} icosahedra in crystalline structures. Furthermore, this polyhedron or its fragments are incorporated in many boron compounds belonging to various types. Amorphous boron can contain discrete groups containing from 2 to 6 bound B_{12} clusters together with structural units of about 100 atoms built of species involving more than 12 boron atoms (with a size of ~15 Å), as well as undeveloped icosahedra and sole atoms in pores.[13, 16–18] Such structure variations affect boron properties, including electronic properties.

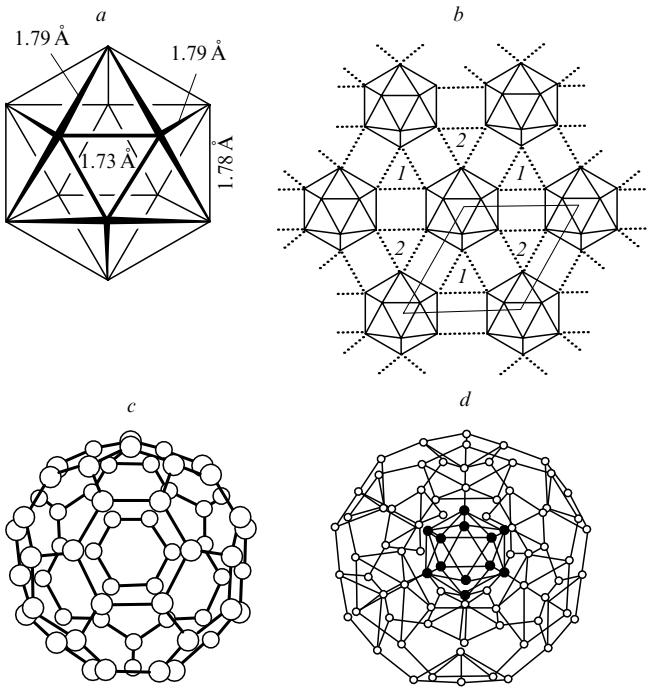


Figure 3. Fragments of structures of elementary boron crystal modifications.[4, 5, 8, 10, 12, 14]

(*a*) B_{12} icosahedron; (*b*) basis layer of B_{12} icosahedra in the structure of α-rhombohedral boron; the numbers *1* and *2* indicate that the triangles are located in different levels (*1*, upper, *2*, lower); (*c*, *d*) structural fragments of β-rhombohedral boron based on a 'giant icosahedron' B_{84} (to provide a better picture, the B_{12} icosahedron existing in the structure is drawn in black circles).

Borides, *i.e.*, compounds and phases in which boron atoms are bound with more electropositive elements (mainly with metals, M), represent a vast class of compounds with diverse compositions and structural types.[4, 5, 8, 10, 12, 19–22] Many of them have a set of valuable physicochemical properties (including mechanical, thermal, corrosion, electrophysical and magnetic properties); a number of phases were found to be superconductors. The crystal-chemical aspects of boride chemistry are generalised in a monograph.[20] The compositions and structure types of binary borides M_mB_n are greatly diverse (Fig. 4). The existence of about 200 such borides were reported.[10] Twenty-four boride compositions have been studied reliably, *viz.*, from M_5B (the metal-rich boride range) to MB_{100} (the boron-rich boride range); however, six variants of the following stoichiometric compositions, the M_2B, MB, MB_2, MB_4, MB_6 and MB_{12} are the most abundant. Moreover, numerous variable-composition phases and solid solutions are known. There are at least six possible configurations of boron atoms in boride structures [10, 22] in which M–B, B–B and M–M bonds are combined in different ways, while boron can be present as single atoms or pairs of atoms, or form zigzag linear structures, branched chains, planar one-dimensional and two-dimensional hexagonal networks, and 3 D cluster fragments (see Fig. 4). In a number of works,[10, 20, 23] binary borides were classified according to the position of the metal in the Periodic table; however, no correlation of boride compositions and structures with the position of the metal could be revealed. For example, hexaborides MB_6 are typical of both alkaline-earth metals and lanthanides and actinides that are quite different from the former; however, these borides have similar structures. Diborides MB_2 are formed by metals of different groups, *viz.*, Mg, Al, Gd, Zr, V, U, *etc.*[4, 10, 20] The nature of chemical bonding in borides is complex. Various combinations of covalent, ionic and metallic bonds exist. Numerous ternary and more complex borides and other compounds, including boron-containing fullerenes and nanostructures, have been obtained and studied.[8, 10, 12, 20, 22, 24] The results of quantum-chemical studies on electronic structures and chemical bond nature in borides were generalised by Ivanovskii and Shveikin.[12, 22]

At least 2500 publications (apart from patents) dealt with problems of chemistry and technology of boron nitride (BN), its crystalline modifications and most important applied properties; Refs 12 and 25–32 are the most interesting. Four crystal modifications of boron nitride are known: two graphite-like modifications, *viz.*, hexagonal (hBN) and rhombohedral (rBN), and two dense diamond-like ones, *viz.*, cubic, or sphalerite-like (cBN) and wurtzite-like (wBN), are present in the phase diagram.[33–35] In lamellar graphite-like modifications, the B and N atoms form σ-bonds with each other; moreover, π-bonding also occurs in the layer planes due to interaction of vacant AOs of the boron atom with the lone electron pair of the nitrogen atom. Bonding between the layers in the hBN structure is also largely determined by the van der Waals and electrostatic interactions of oppositely charged boron and nitrogen atoms in layers located one above another (see Fig. 4 *f*). The bonding of the boron and nitrogen atoms with the tetrahedral coordination in cBN occurs due to the interaction of sp^3-hybrid states. The electronic structure of boron nitride was studied comprehensively; see, *e.g.*, Refs 12 and 36–39.

The fundamentals of the chemistry of boron halides are described in a number of reviews.[10, 40, 41] Covalent trihalides

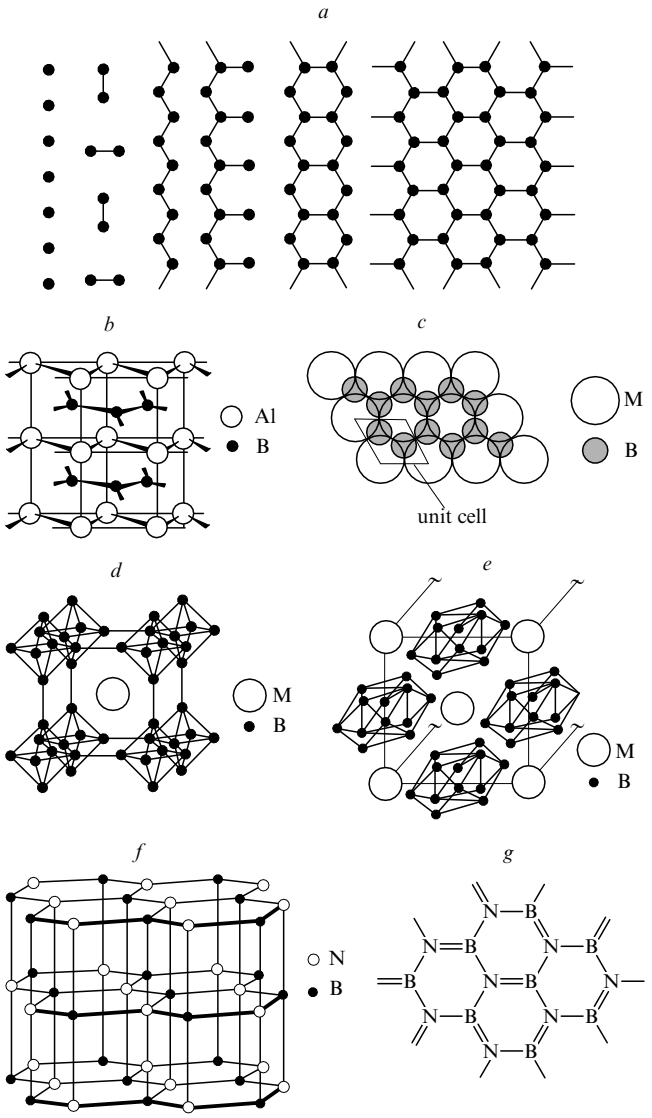
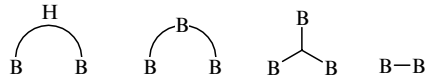


Figure 4. The main structural motives of certain metal borides and hexagonal boron nitride (hBN).
(*a*) shapes of ideal boron atom bonding in metal-rich borides;[10,20,22] (*b*) the AlB_2 crystal structure characteristic of many other diborides;[10,20] (*c*) hexagonal layers of B and M atoms in MB_2 structures; (*d*) cubic structure of metal hexaborides MB_6 containing octahedral clusters of boron atoms;[4,10,22] (*e*) cuboctahedral B_{12} clusters in the structures of dodecaborides MB_{12};[10] (*f*, *g*) lamellar structure of hBN and bonding of B and N atoms in layers.[4,10]

BF_3, BCl_3, BBr_3 and BI_3 are the most typical. Their molecules are characterised by planar trigonal structures with D_{3h} symmetry; sp^2-hybridisation of the 2s-, $2p_x$- and $2p_y$-AOs of the boron atom occurs in these molecules, whereas the $2p_z$-AO remains vacant.[10,40] Therefore, boron trihalides are strong Lewis acids (electron acceptors) that form adducts of the type $L \cdot BF_3$ with Lewis bases (L) (see Refs 42–44). Higher boron halides are also of interest for scientists;[45,46] these include, *e.g.*, B_2F_4 and B_3F_5, clusters such as B_8Cl_8 and B_8F_{12} and the icosahedral *closo*-$B_{12}F_{12}^{2-}$ anion.

The chemistry of boron hydrides and their derivatives is currently matter of intense development. Its fundamentals were established in 1912 in the classical studies by Stock, which he generalised in a monograph.[47] In 1920–1940s, boranes were considered as some kind of 'chemical exotics', as their stoichiometry and the nature of chemical bonds in them could not be rationalised in terms of the classical electronic valence theory. It is of note that the chemistry of boranes and the principles of the valence theory (Lewis' octet theory of bonding electron pairs) appeared almost simultaneously; however, the former turned out to be an opposite of the latter. A rapid development of boron hydride chemistry began in the 1950s. Of note are two types of structures and compositions of the borane systems. The first one includes the simplest systems, such as borane (BH_3), $BH_3 \cdot L$, the tetrahydroborate anion (BH_4^-) and its derivatives, *e.g.*, diborane(6) (B_2H_6). The second type, which is extraordinarily abundant, includes higher boron hydrides and their cluster derivatives, *e.g.*, B_5H_9 and $B_{10}H_{14}$; substituted decaboranes $B_{10}H_{12}L_2$; *closo*-borate anions $B_{10}H_{10}^{2-}$, $B_{12}H_{12}^{2-}$ (of the $B_nH_n^{2-}$ type); carboranes $B_{n-2}C_2H_n$, including *ortho*-, *meta*- and *para*-carboranes(12) ($B_{10}C_2H_{12}$) and their anionic derivatives $B_9C_2H_{12}^-$; 'sandwich'-like complexes of transition metals with the composition $[M^{III}(\eta^5\text{-}B_9C_2H_{11})_2]^-$; metalloboranes and metallocarboranes, *e.g.*, $Sn^{II}B_9C_2H_{11}$; skeletal isomers of the heteroatomic cluster $(C_5H_5)_2Co_2^{III}B_8C_2H_{10}$; thia-*nido*-borane clusters B_9SH_{11}, $B_9SH_{12}^-$, $B_9SH_{11} \cdot L$; borane polymers, and many other compounds.[4,10,46–63] Figures 5 and 6 show schematically the main bond types and examples of structures typical of borane systems. The structures of such compounds (see Fig. 5) are mainly formed with involvement of such bonds as B—H (two-centred terminal σ-bond), B—B (two-centred bond, *e.g.*, in $B_5H_8-B_5H_8$), B—H—B (three-centred bridging bond in B_2H_6 and other boranes), B—B—B (three-centred triangular bond, deltahedron in clusters), BBB (three-centred central bond), M—H—B—H (three-centred bridging heteroatomic bond, *e.g.*, in $Zr[BH_4]_4$).



B = BH.

It is impossible to describe borane clusters in terms of two-centred bonds due to electron deficiency. The concept of a two-electron three-centred bond in boranes was introduced by Longuet-Higgins[64] and developed in the Lipscomb topological system,[65–67] which resulted in the formulation of the Wade '$2n + 2$' rule for the calculation of 'skeletal' electrons that perform bonding in a cluster polyhedron. If one knows the number of 'skeletal' electrons, it is possible to explain and predict the structures of cluster systems in terms of the topology of polyhedra and to systematise such systems.[56,68–70] These concepts serve as a base for classifying cluster structures into *closo*, *nido*, *arachno* and *hypho* types; they are also taken into consideration in the prediction of ways for synthesising new compounds. Yet another, exceptionally important feature of deltahedral borane clusters is that many of them are three-dimensional aromatic systems. The concept of three-dimensional aromaticity and even superaromaticity was introduced by Hoffmann and Lipscomb back in 1962[71] and was subsequently developed in a number of publications.[4,46,52,57,72–75] Such properties of borane clusters as delocalisation of electrons over MOs,[76] chemical stability and specific reactivity[77] are related to aromaticity. Like benzenoid cyclic aromatic systems, different types of three-dimensional borane cluster structures are characterised by high exaltation values‡ of diamagnetic susceptibility[75,78,79] and polarisability. The nature of bonds formed by M atoms in metalloboranes is a matter of discussion, as electron density can be distributed between a metal and aromatic clusters in different ways.[56,58,80] It is undoubtedly interesting to use experimental methods that reveal electronic structures in studies of the nature of bonds in boron hydrides. Until now, the available reviews have covered this subject insufficiently.

‡ Exaltation of diamagnetic atomic susceptibility is the increase in the absolute diamagnetic susceptibility upon inclusion of the atom in an aromatic system.

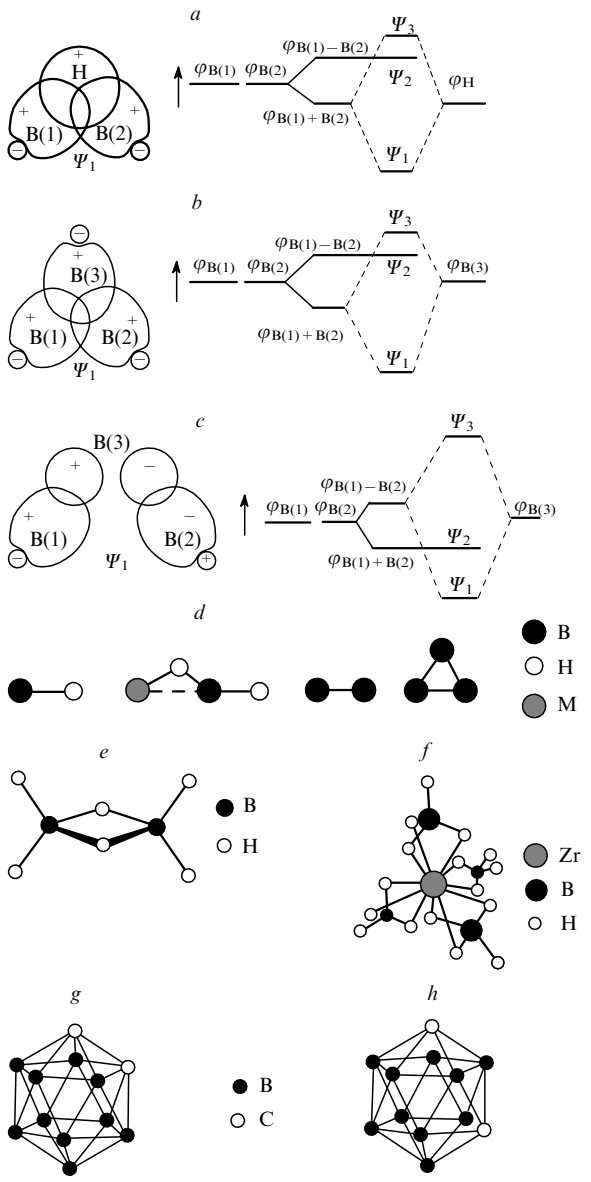
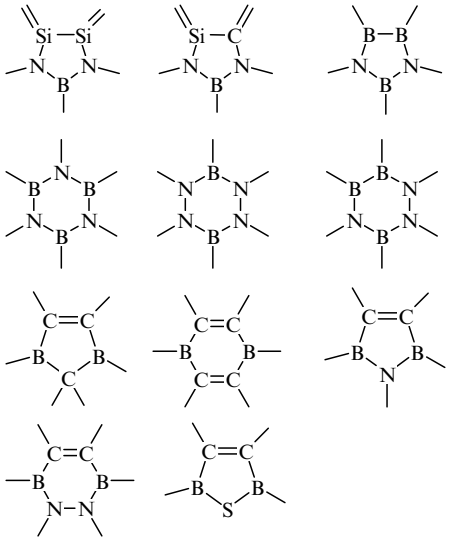


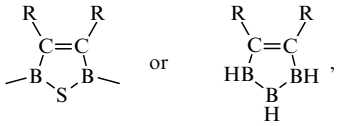
Figure 5. Bond type characteristics of boranes and their derivatives.[4, 10, 58, 64–67]

(*a*) Formation of a B—H—B three-centre bridging bond and schematic representation of the relative energies of three MOs; (*b*) same for central BBB bonds; (*c*) same for open B—B—B bonds; (*d*) types of bonds and structure fragments, including the heteroatomic M—H—B—H bridging bond and a triangular element of a BBB deltahedron; (*e*) structure of diborane(6) molecule incorporating B—H bonds and a B—H—B bridging bond; (*f*) structure of zirconium tetrahydroborate $[Zr(BH_4)_4]$ molecule with heteroatomic ≡Zr—H—B—H bridging bonds; (*g*, *h*) closed deltahedral clusters consisting of B and C atoms in *ortho*- and *meta*-carboranes(12), respectively.

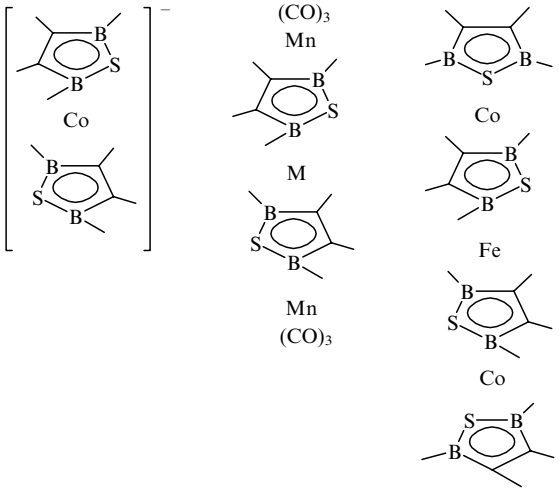
The chemistry of heterocyclic boron compounds is vast. These compounds are characterised by heteroatomic structures containing mainly from 4 to 6 atoms in a ring, systems of fused boron heterocycles and polymers.[10, 81–87] However, no molecular cyclic systems consisting exclusively of boron atoms (similar to cyclohexane, benzene and naphthalene molecules) are known. Along with B atoms, the rings can contain C, O, N, P, Si and S atoms in various combinations. A scheme of MOs upon interaction of B and N atoms in heterocycles is shown in Fig. 7.



Ligands at the ring-forming atoms mainly include organic substituents (alkyls, aryls) and halogens that also stabilise the system. Certain five-membered heterocycles, *e.g.*,



are aromatic and form mononuclear and polynuclear mono- and polymetallic 'multi-decker' 'sandwich'-type complexes with transition metals (Fe, Co, Ni, Cr, Ru) in which planar B_2SC_2, B_3C_2 and other rings serve as bidentate ligands.[61, 86, 88]



M = Fe, Co, Ni.

The nature of chemical bonding in cyclic structures, especially in boron complexes, is rather complex. This involves vacant $2p_z$-AOs of boron, which interact with lone electron pairs belonging to the AOs of other atoms in rings (N, P, S, *etc.*) with partial π-bonding.

By now, the chemistry of organoboron compounds has evolved into an extensive field of science that studies the laws of formation, reactivities, structures and properties of compounds and systems containing =B—CR= bonds with consideration of modern concepts on the electronic nature of bonds.[84, 85, 89, 90]

To a certain extent, the data considered above reflect the complex structure of boron compounds and the diversity of chemical bond types therein. Therefore, the use of experimental methods, such as X-ray emission spectroscopy, X-ray photoelectron spectroscopy and UV photoelectron spectroscopy, com-

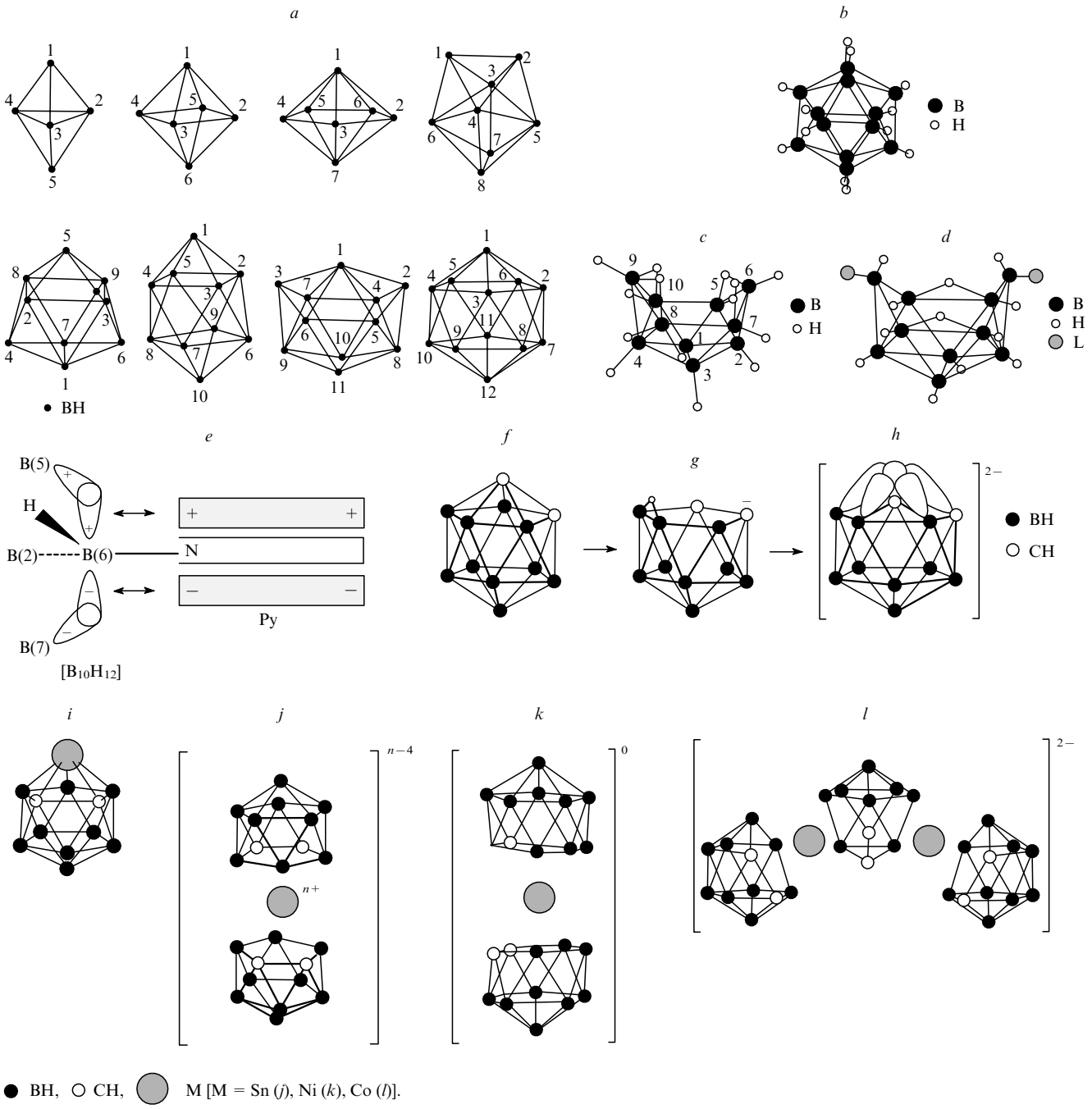


Figure 6. Schematic structures of borane clusters and their derivatives.[4, 10, 46, 52, 54, 56, 68]
(*a*) Cluster-type *closo*-anions $B_nH_n^{2-}$ ($n = 5-12$); (*b*) a $B_{12}H_{12}^{2-}$ anion; (*c*) a decaborane(14) ($B_{10}H_{14}$) molecule; (*d*) a molecule of the 6,9-$B_{10}H_{12}L_2$ adduct; (*e*) interaction of the MOs of boron atoms in the $[B_{10}H_{12}]$ cluster with those of nitrogen atoms in $B_{10}H_{12}Py_2$; (*f*, *g*, *h*) *ortho*-carborane(12) and its anionic derivatives $B_9C_2H_{12}$, $B_9C_2H_{11}^{2-}$, respectively; (*i*) $SnB_9C_2H_{11}$ metallocarborane; (*j*) 'sandwich' structure of tin bisdicarbollyl anionic complex; (*k*) structure of the $[Ni^{IV}(B_9C_2H_{11})_2]^0$ complex; (*l*) structure of the $[(1,2\text{-}B_9C_2H_{11})Co^{III}(B_8C_2H_{10})Co^{III}(1,2\text{-}B_9C_2H_{11})]^{2-}$ complex.

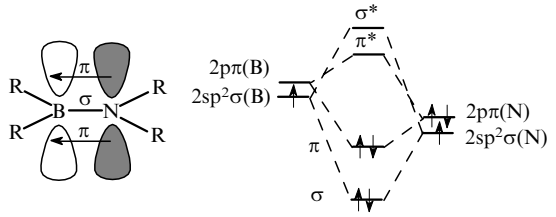


Figure 7. Scheme of AO interaction and qualitative scheme of MOs for the interaction of boron and nitrogen atoms in heterocycles with partial π-bonding.[83]

bined with modern quantum-chemical methods for calculation of electronic structures, allows a deeper insight into the nature of chemical bonds in boron compounds.

III. The physical bases of X-ray spectroscopy

The principles of the XPS, UPS, XES and XAS methods and their experimental bases have been covered in numerous publications, starting from the classical monographs by Blokhin[91] and Siegbahn *et al.*[92] These principles and the experimental techniques for their implementation have subsequently been developed in detail and used to study various compounds.[42, 93–103] It should be noted

that the majority of works on this subject have been carried out in the 1970s and in the early 1980s, when these methods were being implemented intensely. The basic theoretical principles of these methods have not changed considerably since that time. Great advances in the hardware implementation of these research methods have been achieved in recent years due to the development of synchrotron radiation (SR) sources.

1. The bases of X-ray photoelectron spectroscopy and UV photoelectron spectroscopy

Let us start our consideration of the physical bases of X-ray spectroscopy from the XPS and UPS methods, since these methods are used to study the process of 'preparation' for a secondary electron transition in an atom, namely, electron photoemission upon impact of ultraviolet (UV) or X-ray photons and formation of a vacancy on one level of an atom or a molecule. The probability of vacancy formation as a function of the excitation irradiation energy is studied using X-ray absorption spectroscopy. In turn, X-ray emission spectroscopy is used to study the decay of such a vacancy; in particular, the latter can be located on an inner atomic shell.

The XPS and UPS methods are based on the Einstein equation for photoeffect:

$$h\nu = IP + E,$$

where $h\nu$ is the energy of a photon (excitation radiation) impacting an atom; IP is the ionisation energy (potential) or the binding energy (E_b) of a valence or an inner electron level of an atomic–molecular system, which is coordinated with the calculated orbital energy; E is the kinetic energy of a photoelectron, which can be measured by an electron speed analyser. UPS employs ultraviolet irradiation for the excitation, whereas XPS employs soft X-ray irradiation. The most common UV sources include the He(I), He(II) and Ne(I) resonance lines (21.2, 40.8 and 16.8 eV, respectively), which allows the energies of outer electrons of atomic–molecular systems to be determined.[42, 94, 96, 98] The sources used in XPS mainly include the MgK_α- (1253.6 eV) and AlK_α-radiation (1486.6 eV).[42, 93, 96, 97, 99, 100] A photoelectron spectrum is the dependence of the number of emitted photoelectrons per unit time, *i.e.*, the line intensity (I), on the ionisation potential (IP) or binding energy (E_b) (the magnitudes of IP and E_b are usually expressed in eV). The measured values of IP or E_b make it possible to reveal the order of energy levels in a molecule, their symmetry, the bonding or antibonding character of separate MOs, and the relative contributions of different AOs of adjacent atoms when a MO is formed (these data are important for understanding various physical and chemical properties of a compound). In order to interpret UPS and XPS spectra of various compounds, it was suggested (with a considerable degree of approximation) to allocate three spectral regions, depending on the electron binding energy.[103] The first region ($E_b \approx 0-15$ eV) characterises structures formed with involvement of electrons from outer valence MOs, which are mainly formed by incompletely filled electrons of valence AOs. The second region ($E_b \approx 15-50$ eV) covers the structures formed by electrons of inner valence MOs (IVMOs). Finally, the third region ($E_b \gtrsim 50$ eV) contains lines reflecting the positions of deep inner (core) AOs. At present, a concept is being developed that IVMOs are considerably involved in chemical bonding along with valence MOs.[103] X-Ray spectroscopy confirms some statements of this concept by shedding light on the very complex actual electronic nature of chemical bonds. It should also be noted that the UPS method is used to study valence shells, whereas XPS is often used to study inner (atomic) shells, though it is used rather extensively to study outer shells as well.

2. X-Ray emission and absorption spectroscopies and their specific features

X-Ray emission and absorption methods provide information about the energy, composition and symmetry of molecular orbitals. The use of these methods for the study of chemical bonds is covered in a number of monographs.[42, 96, 99, 101]

Let us consider the physical principles of the XES and XAS methods. X-Ray emission radiation appears to be due to transitions of electrons from outer occupied levels of a molecule to inner atom-like levels that contain vacancies, which, in turn, are formed due to interaction of the molecules with a beam of high-energy electrons or upon irradiation by X-ray photons. X-Ray absorption spectra reflect transitions of electrons from an inner level to outer vacant levels of a molecule caused by incidence X-ray radiation. The main distinctive feature of these processes is that these are involved in both emission and absorption electron transitions of an inner level; the electrons on this level contribute only slightly to the chemical bond and have an almost atomic character. On the other hand, outer MOs form a system of orbitals common to the entire molecule. One can find the ionisation potential of a valence MO (IP_i) by determining the energy of an X-ray photon, which is equal to the energy of electron transition between two levels, *viz.*, an outer valence level (i) and an inner level (k), $h\nu = E_{ik}$, and given the ionisation potential of the inner MO (IP_k) (which is obtained by XPS):

$$IP_i(\mathrm{MO}) = IP_k(\mathrm{AO}) - E_{ik}.$$

Experimental values of IP_i(MO) are also provided by UPS. Hence, using the above relationship as the base, one can compare the X-ray and photoelectron spectra in a single energy scale of ionisation potentials (this operation was called matching).[96] Such a combined use of XES, UPS and XPS allows much more precise identification of specific spectral lines. However, X-ray emission spectra of different elements of a chemical compound under study can provide not only the values of MO energies but also data on the contributions of separate AOs of these elements to these values. X-Ray absorption spectra provide similar data about vacant MOs. As noted above, XES and XAS spectra can be used not only to study the energy spectrum of a molecule but also to analyse the composition of molecular orbitals, namely, to determine the squares of the coefficients at the atomic wave functions constituting an MO. To illustrate this, Fig. 8 shows a qualitative scheme of X-ray transitions from two MOs, i and j, to inner 1s-levels of boron and carbon atoms (taken as examples) within a polyatomic molecule. (It should be remembered that the short notation of X-ray spectra includes the element symbol, the level to which the electron transition occurs, and — for emission spectra — a Greek letter indicating the particular transition. In the case of absorption spectra, no Greek letter is specified.) As one can see from Fig. 8, transitions from valence MOs i and j to the same inner level, *e.g.*, B1s, give X-ray BK_α-spectral lines whose intensity ratio is equal to the ratio of squares of the contributions of the 2p-AOs of boron ($I_i/I_j = c^2_{i\mathrm{B2p}}/c^2_{j\mathrm{B2p}}$). C$K_\alpha$-Spectral lines can be analysed in

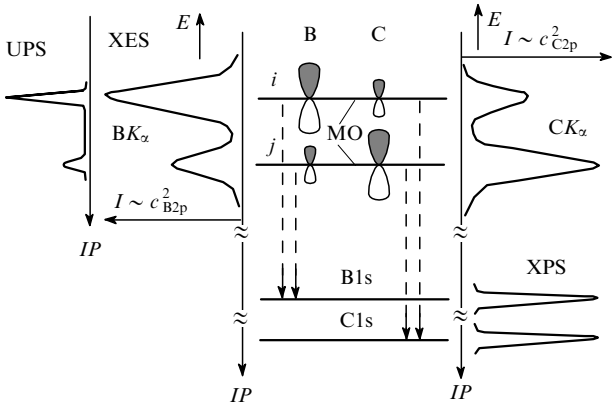


Figure 8. Scheme of X-ray transitions in the molecule and their identification. See the text for explanations.

a similar way; furthermore, more valence and inner levels can be taken as examples. A detailed analysis of this method for the determination of energy positions of MOs and their compositions is presented in a number of publications [42, 96, 101] where its scope and limitations are discussed. It should be noted that the K_α-spectra of B, C, N, O and F atoms considered in this review allow one to determine the contributions of 2p-AOs of these atoms to MOs of chemical compounds; the K_β-spectra of P, S and Cl atoms allow the determination of the contributions of 3p-AOs to MOs, the $L_{2,3}$-spectra of these atoms provide the contributions of 3s- and 3d-AOs, and finally, the L_α-, L_β-spectra of Fe, Co and Ni atoms provide the contributions of the 3d-AOs.

The instruments and procedures used to obtain X-ray emission and absorption spectra have been described in detail in a number of monographs.[42, 91, 95, 96, 99, 101, 104] The scheme of an X-ray spectrometer is shown in Fig. 9. The X-ray emission radiation of a compound under study, that can be either in a solid or gaseous state, is excited by electrons or photons. The induced radiation passes through a number of diaphragms and falls on the dispersing element and, after reflection from the latter, on the detector. Expansion of the X-ray radiation from the compound into a spectrum by the dispersing element followed by recording of the spectrum can give the dependence of the radiation intensity on the wavelength or photon energy (in eV). X-Ray absorption spectra are obtained as follows. A sample to be studied is placed in the way of X-ray radiation and the attenuation/absorption factor (defined as the logarithm of the ratio of the beam intensity that has passed through the sample to the initial beam intensity) is determined as a function of the energy of the monochromatic exciting radiation. In the case of samples non-transparent to soft X-ray irradiation, X-ray absorption spectra are recorded in the electron yield mode (complete or partial yield, or yield of Auger electrons as a function of energy discrimination of detected electrons).[104] Synchrotron radiation, whose intensity is many orders of magnitude higher than that from X-ray tubes, is increasingly used at present to excite X-ray transitions in chemical systems.[105–107]

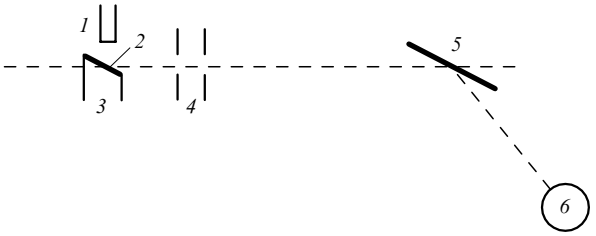


Figure 9. Schematic diagram of an X-ray spectrometer.
(*1*) Electron gun or primary radiation (photon) source; (*2*) compound under study; (*3*) sample holder (secondary anode); (*4*) system of apertures; (*5*) dispersing element (analyser crystal or diffraction lattice); (*6*) detector.

The information provided by X-ray absorption spectra can also be obtained from electron energy loss spectra (EELS).[108] The essence of this spectral method is as follows: as a result of inelastic collision of monochromatic electrons with molecules under study, one of their inner electrons passes to one of the available vacant levels, whereas the loss of the energy of the incidence electron is equal to the energy of this transition. Having determined the electron energy before the collision and that after the collision using an energy analyser, one can plot the energy spectrum of transitions from different inner molecular levels to vacant orbitals.[108, 109] Inelastic scattering of hard X-ray irradiation (X-ray Raman scattering) can be used in a similar way.

A specific feature of chemical bonding in many boron-containing compounds is that it involves donor–acceptor interactions. The formation of a donor–acceptor bond between two molecules (*e.g.*, $NX_3 \cdot BY_3$, where X, Y = H, Hal, Alk *etc.*) occurs

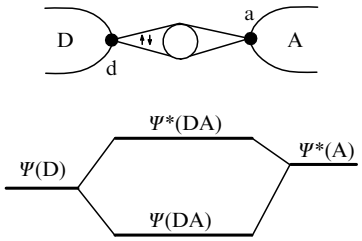


Figure 10. Scheme of donor–acceptor interaction in the two-level model approximation. See the text for explanations.

due to the electron density transfer from the highest-energy occupied orbital of the donor to the lowest-energy vacant orbital of the acceptor (for more details, see Refs 110–112).

Donor–acceptor interaction in the two-level model approximation is demonstrated in Fig. 10. A system under study contains two valence-saturated molecules, *viz.*, a donor (D) and an acceptor (A). The highest occupied MO (HOMO) of the donor contains a lone electron pair localised on the 'd' atom (see Fig. 10). The wave function of this orbital, $\Psi(D)$, consists of one wave function of the 'd' atom, $\psi(d)$. The lowest unoccupied MO (LUMO) of the acceptor is localised on the 'a' atom. Its wave function $\Psi^*(A)$ (here and below, vacant orbitals are marked with asterisks) also consists of one wave function of the 'a' atom of the acceptor molecule, *i.e.*, $\psi^*(a)$. It is sometimes called a lone hole pair. Thus, the HOMO of the 'D' molecule and the LUMO of the 'A' molecule are similar to the AOs of the 'd' and 'a' atoms, respectively. Interaction of the 'D' and 'A' molecules through the 'd' and 'a' atoms results in an occupied bonding orbital with the wave function $\Psi(DA)$ and a vacant antibonding orbital with the wave function $\Psi^*(DA)$:

$$\Psi(DA) = c_d\Psi(D) + c_a\Psi^*(A) = c_d\psi(d) + c_a\psi^*(a),$$

$$\Psi^*(DA) = c_d^*\Psi(D) - c_a^*\Psi^*(A) = c_d^*\psi(d) - c_a^*\psi^*(a),$$

where c_d, c_a, c_d^* and c_a^* are expansion coefficients of the MOs over the AOs. The degree of electron density transfer from the donor to the acceptor, in both the main and excited states, depends on the values of the squares of these coefficients.

Let us consider how the donor–acceptor interaction manifests itself in X-ray spectra. The HOMO of the donor molecule (lone electron pair) is described by the wave function of the highest occupied AO of the donor atom. The expansion coefficient of the AO in the MO is equal to unity ($c_{ij} = 1$). The donor molecule does not have any other orbital with such a high contribution of this AO. Naturally, inasmuch as $I \sim c_{ij}^2$ (see Fig. 8), the electron transfer from the HOMO gives the most intense line in the X-ray spectrum. In the two-level model approximation, the HOMO of the new compound DA resulting from the formation of a donor–acceptor bond is described by a wave function consisting of two AOs, *viz.*, that of the 'd' atom of the 'D' molecule and that of the 'a' atom of the 'A' molecule. Accordingly, the participation coefficient of the AO of the 'd' atom of the donor molecule 'B' becomes less than unity. Hence, the relative intensity of the X-ray line originating from the electron transfer from the MO of the DA molecule to the inner level of the 'd' atom of the same molecule also decreases. It is assumed that deeper MOs of both the donor and acceptor do not change, that is, the bond formed between the molecules does not introduce considerable disturbance, and their electrons are not involved in the formation of the chemical bond. As a result, the structure and intensity of the rest of the X-ray spectrum change quite insignificantly. In such a case, filling of the LUMO under consideration changes the intensities in the X-ray absorption spectra of the acceptor molecule within the DA adduct. It should be noted that the approach described above is

rather approximate and that it is useful for illustration purposes only.

IV. X-Ray spectroscopy and electronic structure of boron compounds

Fundamental X-ray spectral studies of boron compounds were carried mostly in the 1960–1970s by a group of physicists from the Leningrad University.[104] The X-ray spectra recorded in the 1930–1940s when the ultra-mild X-ray spectroscopy was in its infancy were limited by the low resolution of equipment and were only descriptive (see the references in the monograph by Maisel *et al.*[99]).

1. Oxide systems

X-Ray studies have been conducted for only a few oxygen-containing boron compounds. The majority of studies dealt with the electronic structure of boric anhydride (B_2O_3). The following spectra were recorded and discussed: emission BK_α-spectra,[39, 93, 104, 113–127] OK_α-spectra[116, 117] and absorption BK-spectra.[39, 104, 115, 122, 123, 128–132]

Extensive application of synchrotron radiation as a source for the excitation of X-ray fluorescence in studies of the electronic structure of B_2O_3 began in the 1990s.[121–125] It was used in a number of studies[122, 123, 128–131] of X-ray absorption spectra of boron. O'Brien *et al.*[121] and Muramatsu *et al.*[122–124] studied the BK_α-emission spectra of boron (Fig. 11) using monochromatic synchrotron radiation. It was found that changes in the energy (or wavelength) of excitation radiation change both the energy positions of single lines and their intensities, and hence the shape of the entire spectrum. The behaviour of the highest-energy structure (the region of ~190–210 eV in the transition energy scale) is characterised by the greatest differences. Having related the energies of emission lines to the values of the energy maxima in the X-ray absorption spectrum (see Fig. 11 *a*), one can say that vacant orbitals (excited state) specifically manifest themselves in the emission spectrum due to reemission transitions. Reemission transitions have first been studied by Fomichev *et al.*[39] The reemission process involves two steps, *viz.*, transition of an electron occurs in the first step, *e.g.*, from an occupied K-shell to a vacant orbital to form a line in the absorption spectrum and reverse transition of the electron to the original level K occurs in the second step, which results in a line in the emission spectrum. Generally, these lines have the same energies if both spectra are compared (see, *e.g.*, Ref. 104). Studies of the behaviour dynamics of reemission lines as a function of the exciting radiation energy revealed the existence of some kind of resonance: if the excitation energy coincides with the energy of electron transition from the K-shell of the boron atom to a vacant orbital, the intensity of the reemission line increases.[123, 124] The theory of resonance excitation was considered in a series of fundamental studies (see, *e.g.*, the monograph by Mazalov *et al.*[96] and references cited therein). It should be noted that a version of X-ray emission spectroscopy which uses resonance excitation is called resonant inelastic X-ray scattering (RIXS) in current literature.

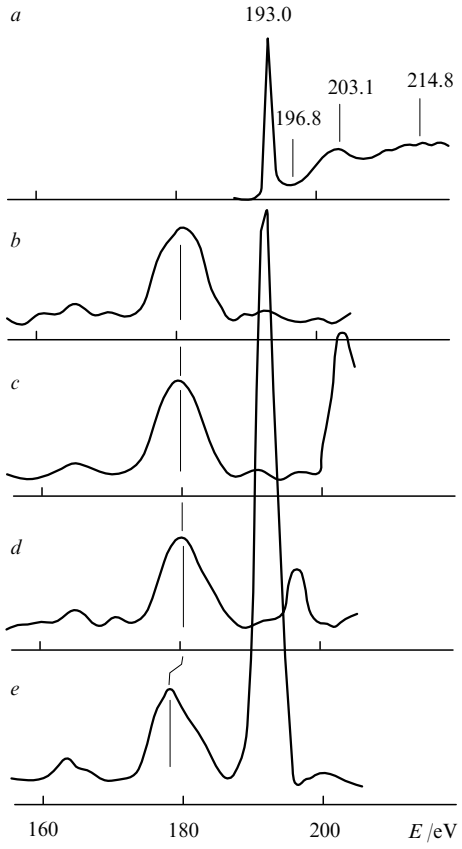


Figure 11. X-Ray absorption spectrum of boron (*a*) and X-ray BK_α-emission spectra of boric anhydride B_2O_3 (*b*–*e*) obtained at different synchrotron excitation energies (E_{hv}).[123]
E_{hv} = 214.8 (*b*), 203.1 (*c*), 196.8 (*d*), 193.0 eV (*e*).

A combined analysis of the K_α-spectra of boron and oxygen and the XPS spectrum of B_2O_3 in the valence band was carried out.[133] All the spectra were reduced to a common energy scale using XPS data. The structure of a particular cluster was considered. Based on X-ray spectra, conclusions on the contributions of the 2p-AOs of oxygen and boron to different levels of the valence band were drawn.

One of the first interpretations concerning boron X-ray emission and absorption spectra was based on quantum-chemical calculations in the CNDO approximation.[134] It was assumed that the symmetry point group of the boron atom's nearest environment in the planar network is D_{3h}. The calculation was first performed for the BO_3^{3-} cluster, *i.e.*, only the first coordination sphere was taken into account; after that, for better fit with experimental X-ray emission and absorption spectra, the BO_3B_3 cluster was calculated, *i.e.*, the second coordination sphere was also taken into account. This is likely to be the only study where X-ray emission and absorption spectral lines of boric anhydride, B_2O_3, are compared with the symmetry and energy parameters of levels calculated by quantum-chemical methods. The Xα-DV (discrete variation) approximation was used to simulate the X-ray BK_α-emission spectrum,[124] though Muramatsu *et al.*[122] reported only the overall spectrum shape but not the energies of the spectrum-forming MOs calculated by the quantum-chemical method. A more detailed approach was used by Kawai *et al.*[135] who reported the energies of the MOs forming the theoretical spectrum and their symmetries; in the case of boric anhydride B_2O_3, they considered the $B_2O_5^{4-}$ cluster (point symmetry group D_{2d}) in which each boron atom is surrounded by three oxygen atoms. However, Kawai *et al.*[135] only studied the X-ray OK_α-emission spectrum.

The X-ray emission and absorption spectra of B_2O_3 reduced to a common energy scale using the binding energies of inner electrons[100] are presented in Fig. 12, which shows XPS spectra in the valence band. The zero on the binding energy scale corresponds to the Fermi level (E_F) of the X-ray photoelectron spectrometer (see Refs 92 and 133). Different spectra were compared using XPS data in the energy region corresponding to inner layers.[100] To identify the structures of these spectra, let us compare different spectra, as has been done by Nakhmanson and Baranovskii,[134] based on data on the electronic structure of the BO_3^{3-} cluster with D_{3h} symmetry. X-Ray OK_α- and BK_α-emission spectra provide data on the contributions of the 2p-AOs of oxygen and boron to the occupied MOs, while the corresponding absorption spectra reflect the structures of vacant orbitals. The low-energy (henceforth, the transition energy scale is implied) e′(σ)-

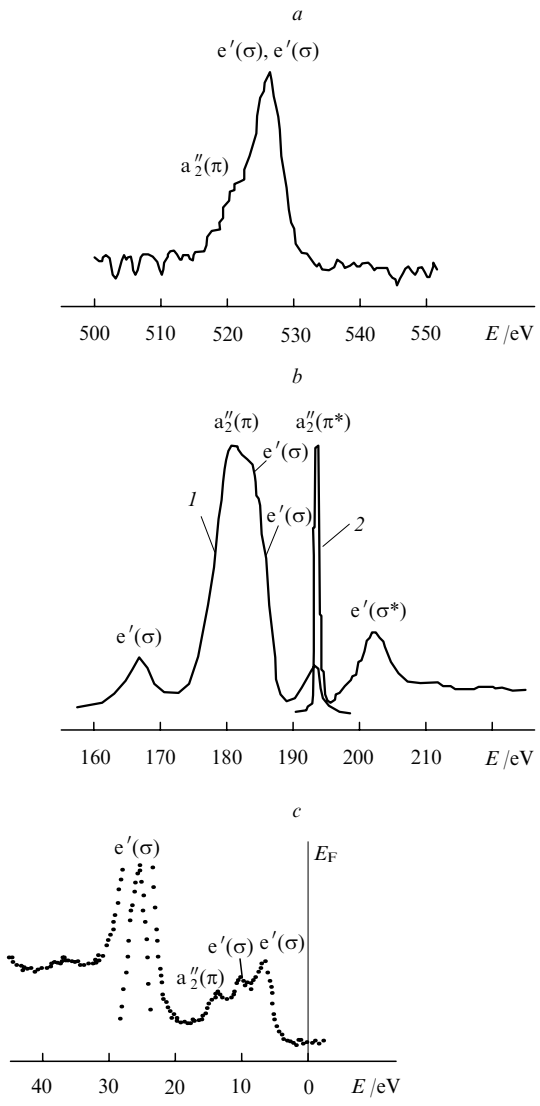


Figure 12. X-Ray OK_α-emission spectrum (*a*),[116] X-ray BK_α-emission spectrum (*b*, spectrum *1*),[115] X-ray spectrum near the radiation B*K*-absorption edge (*b*, spectrum *2*)[131] and X-ray photoelectron spectrum in the B_2O_3 valence band (*c*).[133]

line of the X-ray BK_α-emission spectrum, which coincides with an intense line in the XPS spectrum (see Fig. 12), matches the MO with e′ symmetry mainly formed from oxygen and boron 2s-AOs. In the X-ray BK_α-emission spectrum, this is manifested due to a small admixture of the B2p-AO. Electrons of this orbital form σ-bonds between boron and oxygen atoms. They are followed by one orbital with a''_2 symmetry (π-bond) and two MOs with e′ symmetry (σ-bond) mainly consisting of boron and oxygen 2p-AOs. They manifest themselves as a low-energy shoulder on the dominant line and as this line of its own in the X-ray OK_α-emission spectrum, and also as a broad intense band in the X-ray BK_α-emission spectrum (see Fig. 12). There is a corresponding broad band consisting of three lines in the X-ray photoelectron spectrum. The first line of the X-ray spectrum near the B*K*-absorption edge of boron, which is identified as a vacant $a''_2(\pi^*)$-MO, matches the highest-energy maximum of the X-ray BK_α-emission spectrum. This provides reasons to assign the latter to a reemission transition line, *i.e.*, electron transition from the excited $a''_2(\pi^*)$-level to a vacancy in the boron *K*-shell. Finally, the last broad line in the absorption spectrum is matched with the antibonding unoccupied e′(σ*)-MO.

The X-ray OK_α-emission spectrum of boron suboxide B_6O was studied.[135, 136] Quantum-chemical calculations of the B_6O structure and of this spectrum were performed in the Xα-DV approximation using a cluster of two triangles, which contained boron atoms in the vertices and oxygen atoms in the centres (B_6O_2). The electronic structures were calculated and the X-ray OK_α-emission spectra were constructed as a function of the distance between the oxygen atoms and hence between the planes in which these triangles are located. Kawai *et al.*[135, 136] chose this distance in such a way that the theoretical and experimental spectra matched most closely and compared it with data on the B_6O structure. An experimental X-ray BK_α-emission spectrum was published earlier,[137] with the spectrum structure studied at different energies of the excitation SI.

The X-ray BK_α-emission spectrum[113, 120] and X-ray OK_α-emission spectrum of H_3BO_3 were obtained.[138] The B*K*-absorption spectra of this compound were recorded in a number of studies,[128, 129, 132, 139] the first of which employed SI. The X-ray absorption spectrum was also reported.[139] The spectra of H_3BO_3 and B_2O_3 are very much alike because the boron and oxygen atoms have the same nearest environment. The identification of maxima in the structures of X-ray BK_α-emission and B*K*-absorption spectra of H_3BO_3 was performed on the basis of calculation of these spectra in the CNDO approximation.[134]

The electronic structures of other oxide compounds of boron were also studied.[113, 120, 128] For example, X-ray emission spectra of boron were recorded and described for $Na_2B_4O_7$,[113] $AlBO_3$, $Be_2(BO_3)OH$, $Mg[(OH)_3BOB(OH)_3]$, $CaB_2Si_2O_8$ and BPO_4.[120] The X-ray absorption spectra of boron for $Na_2B_4O_7 \cdot 10\,H_2O$, $NaBO_3 \cdot 4\,H_2O$, $Zn[B_2O(OCOMe)_5]_2$ and BPO_4 were obtained using SI.[128]

2. Elementary boron, borides and boron carbide

Numerous studies deal with X-ray emission (Refs 93, 104, 113–117, 122, 126 and 140–145) and X-ray absorption spectra of elementary boron.[104, 115, 122, 129, 130, 140, 143, 144] Although several modifications of crystalline and amorphous boron exist, their X-ray spectra differ insignificantly. The most considerable 'chemical' effects are observed in the BK_α-spectra on transition from elementary boron to its oxide and nitride (see Sections IV.1 and IV.3). The spectra of B, B_2O_3 and BN show noticeable differences: a considerable low-energy shift of the main band is observed for B_2O_3 and BN (by 2.72 and 2.45 eV, respectively, with respect to B); in addition, the spectra of B_2O_3 and BN contain new lines in comparison with the spectra of elementary boron. These include a low-energy line (165.4 eV in the spectrum of B_2O_3 and 169.0 eV in the spectrum of BN), which originate probably from electron transitions from the MO mainly containing the B2s-AO (with a small contribution of the B2p-state) to the *K*-shell of the boron atom containing a vacancy, as well as the maxima which appear due to reemission transitions (191.4 and 190.0 eV for B_2O_3 and BN, respectively).[93] These features may be related to changes in both the chemical environment of the boron atom and the character of binding (see, *e.g.*, Ref. 93). A comparison of X-ray emission and X-ray absorption spectra of amorphous boron allowed the band gap width to be evaluated.[140] Sobczak and Persy[144] reduced the BK_α-emission and B*K*-absorption spectra, as well as the photoelectron spectrum in the valence band, to a common energy scale using the energies of inner B1s-electrons. They also presented an X-ray isochromate[144] of elementary boron whose structure compares with that of the XAS spectrum (the method to obtain isochromates was described, *e.g.*, by Maisel *et al.*,[99] who also gave references to early X-ray spectroscopic studies). Results of studies on the electronic structures of different modifications of elementary boron were generalised in the monograph by Ivanovskii and Shveikin.[12]

The monograph by Zhurakovskii[146] should be considered among the first works on the electronic structures of borides M_nB_m (where M is a metal) studied by X-ray spectroscopy. He presented a large number of X-ray spectra and related them to

parameters that characterise the electronic structures of compounds (the energies and relative intensities of spectral lines). The results of more recent studies on the electronic structures of metal borides were generalised in the monograph by Ivanovskii and Shveikin.[12]

Studies on medium-temperature superconductivity carried out in the past decade showed that this property is inherent in MgB_2 as well.[147] Its electronic structure was studied by various physical methods, including XES and XAS.[148]

The X-ray BK_α-emission spectra,[104, 113–116, 118, 120, 126, 149, 150] CK_α-emission spectra[116] and X-ray absorption spectra[104, 115, 130, 149, 150] of boron carbide B_4C were recorded and described. The X-ray BK_α-emission and BK-absorption spectra of $B_{10}C$ and $B_{11}C$ were studied,[150] and the X-ray BK_α-emission spectrum of $B_{12}C_3$ was published.[117] Unfortunately, traditional analysis of these spectra based on calculation results was not carried out in these studies, hence identification of spectral lines was not performed either.

3. Boron nitrides and other binary compounds

The X-ray BK_α-emission spectra of boron nitrides (Refs 39, 93, 104, 113–118, 120, 121, 124–126, 133, 136, 140, 151–155) their X-ray BK-absorption spectra,[39, 104, 115, 122, 130, 140, 151–153, 156, 157] NK_α-emission spectra[93, 104, 116–118, 126, 133, 140, 151–154] and NK-absorption spectra were studied.[104, 131, 151–153, 156] Considerable attention was given to the study of the structures of these spectra. For example, it was shown that admixtures of elementary boron or a boron oxide film affect the X-ray BK_α-emission spectrum of hBN.[39] Furthermore, the existence of several modifications of crystalline boron nitride gave grounds for studying the composition of a BN sample in order to find out whether it contained only one or several modifications.[154] The X-ray spectra of boron nitride modifications, cBN and hBN, differ markedly. Joyner and Hercules[133] studied X-ray emission spectra along with the photoelectron spectrum in the valence band of hBN.[133]

As noted above (see Section III.2), SI is currently being used ever more often to obtain X-ray spectra. This irradiation source was also used to study the emission and absorption X-ray spectra of boron nitride.[121, 122, 124, 125, 130, 131, 158–170] In a number of experiments, emission spectra of boron nitride were recorded with excitation of X-ray fluorescence by monochromatic (or quasi-monochromatic) SI. The X-ray fluorescence spectra obtained in this way differ in the energy positions of separate lines and their relative intensities depending on the wavelength of the excitation line. This effect was observed for X-ray lines of both BK_α- and NK_α-emission.[121, 122, 124, 158–165] In some works,[124, 159, 161] monochromatic radiation was used to study the high-energy structures of spectra or lines of reemission transitions (*cf.* Section IV.1, analysis of the X-ray spectra of B_2O_3). The intensity of a line corresponding to reemission transition increases abruptly at a certain energy of the excitation photon.

The polarisation character of X-ray emission spectra of hBN single crystals and changes in the bands of these spectra (their positions and intensities) for different directions of the radiation exit from single crystals with respect to particular crystallographic orientations were studied.[171–174] Synchrotron radiation was used as the irradiation source in many studies.[37, 158, 167, 175–180] The orientation emission effect was also used to determine the symmetry of vacant orbitals that manifest themselves in absorption spectra.[167, 177–180] Electron energy loss spectroscopy was used to study the orientation effects in hBN crystals.[181, 182] The dependence of the reflection factor of ultrasoft X-ray irradiation by hBN near the K-edge of boron absorption on the grazing incidence angle was studied.[183, 184] In this study, reflections from two crystal faces cut in parallel and normally to its main symmetry axis were measured successively. These spectra agree satisfactorily with those obtained in the electron yield mode (see Section III.2).

One of the first calculations of boron nitride was carried out for hBN using the CNDO method with the first (the BN_3^{6-} cluster) and second (BN_3B_6) coordination spheres taken into account.[134] As expected, the results are similar to X-ray spectroscopic experimental data provided that the effect of the second coordination sphere is taken into account. The main specific features of X-ray emission and absorption spectra are related to the structure of the nearest environment of an excited atom, which explains the differences between the X-ray spectra of different BN modifications. Based on calculations of the electronic structure in the Xα-DV approximation, a theoretical X-ray BK_α-emission spectrum of boron nitride was obtained.[122] Data on calculations on the electronic structure of boron nitride were summarised and compared to experimental spectra in certain monographs.[12, 185] The most recent achievements in this field are reported in Refs 186–192.

This was the general survey of X-ray studies on the electronic structure of boron nitride. Let us consider some of its aspects more specifically and see how chemical bond features manifest themselves in the X-ray spectra. Figure 13 *a*,*b* shows the X-ray spectra of the hexagonal and cubic modifications of boron nitride, respectively. The X-ray BK_α- and NK_α-emission spectra were taken from Refs 151 and 152, while the BK- and NK-absorption spectra were taken from Ref. 131. All the spectra refer to a common energy scale relative to the Fermi level, taking into account the binding energies of inner B1s- and N1s-electrons obtained by XPS;[100] they are compared with photoelectron spectra of boron nitride in the valence band.[193, 194] The X-ray spectra of hexagonal boron nitride are interpreted on the basis of results of CNDO calculations[134] for the BN_3^{6-} cluster (symmetry point group D_{3h}) and MNDO calculations (MOPAC-60 software) for a hypothetical isolated BN molecule (symmetry group $C_{\infty v}$). The results of the latter are shown in Fig. 14. MNDO calculations for such a molecule give quite a moderate qualitative picture of the electronic structure of boron nitride as a polyatomic system that has different modifications, but maintains its main features. Passage from an isolated BN molecule to a polyatomic system results in dithering of the MO into a band whose description requires calculations within the zone theory of solids or quantum-chemical calculations of polyatomic clusters. If hBN is considered with the nearest environment taken into account, then the e′-MO is the orbital whose electrons form the σ-bond in the layer plane (hBN is considered as a lamellar structure). Molecular orbitals of this symmetry are built of $2p_x$- and $2p_y$-AOs of boron and nitrogen; the MOs with the a_2'' symmetry are built of $2p_z$-AOs and are responsible for the π-type chemical bond in the layer normal to the network plane. The deepest valence level is comparable with the low-energy line of X-ray BK_α-emission spectrum of low intensity (see Fig. 13); no similar line was found in X-ray NK_α-emission spectra presented in Refs 151 and 152. Only Hayasi[116] succeeded in obtaining a low-intensity maximum with a transition energy of ~ 377 eV. A comparison of both of these low-energy lines in the X-ray BK_α- and NK_α-emission spectra show that their energies match each other and the energy of the most intense line in the XPS spectrum.[193] According to quantum-chemical calculations, these lines can be related to the level corresponding to the σ-bond and mainly consisting of the 2s-AOs of boron and nitrogen. They appear in X-ray BK_α- and NK_α-emission spectra because the e′(σ)-MOs contain an admixture of 2p-AOs of the same atoms (see Fig. 13). An increase in the transition energy produces intense maxima with fine structure in X-ray BK_α- and NK_α-emission spectra; these maxima coincide if the spectra are superimposed. It is suggested to match the intense BK_α-band with the a_2''-MO and to match the high-energy shoulder successively with two orbitals with e′ symmetry.[134] However, the results of MNDO calculation (see Fig. 14) and data of studies on polarisation effects in X-ray emission spectra[37] (see Fig. 13) suggest that a somewhat different order of these orbitals should be assumed: as the transition energy increases, two MOs with e′ symmetry are followed by a MO with a_2'' symmetry (see Fig. 13). The fact that the maxima in X-ray BK_α- and NK_α-emission spectra and XPS spectra coincide in the valence band if a comparison is made using the energy positions of inner orbitals allows these

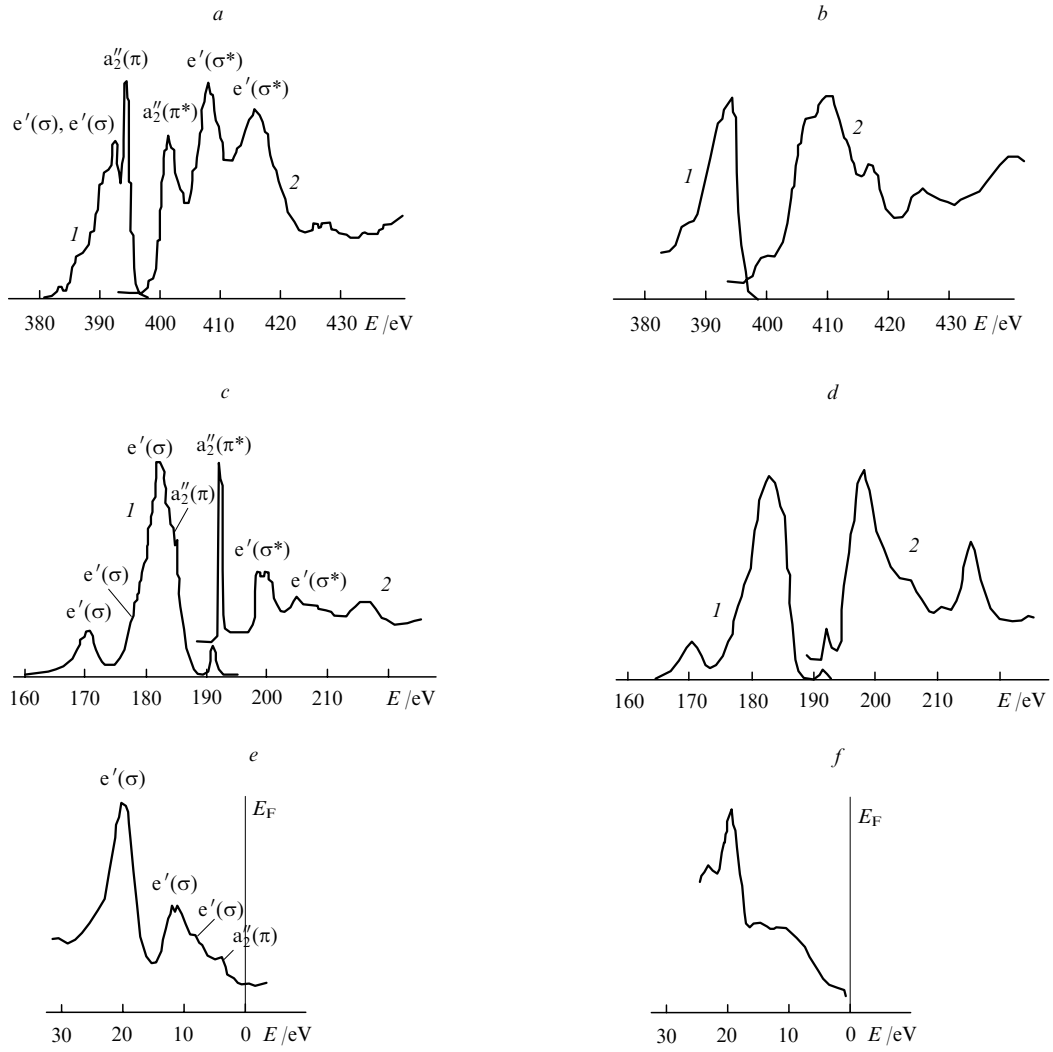


Figure 13. X-Ray NK_α- (*a*, *b*) and BK_α-emission spectra (*c*, *d*) (spectra *1*) [151, 152] and N*K*- (*a*, *b*) and B*K*-absorption spectra (*c*, *d*) (spectra *2*) [131] and photoelectron spectra (*e*, *f*) [193, 194] in the valence band of hexagonal (*a*, *c*, *e*) and cubic (*b*, *d*, *f*) boron nitride.

X-ray spectra to be interpreted as well (see Fig. 13). According to CNDO calculations, the first vacant orbital [134] has a_2'' symmetry and corresponds to a narrow line in the X-ray B*K*-absorption spectrum (see Fig. 13) and to a distinct line in the X-ray N*K*-absorption spectrum.[131] The same conclusion can be drawn based on the fact that the line positions coincide when the X-ray B*K*- and N*K*-spectra are superimposed. It is also evident from Fig. 13 that the first low-energy line in X-ray absorption spectra coincides with the reemission line in the X-ray BK_α-emission spectrum, which thus can be related to the lowest vacant $a_2''(\pi^*)$ level. The two next vacant MOs with the e' symmetry manifest themselves in X-ray absorption spectra as two distinct lines [131] (see Fig. 13).

As noted above, studies of orientation (polarisation) effects have played an important role in the interpretation of boron

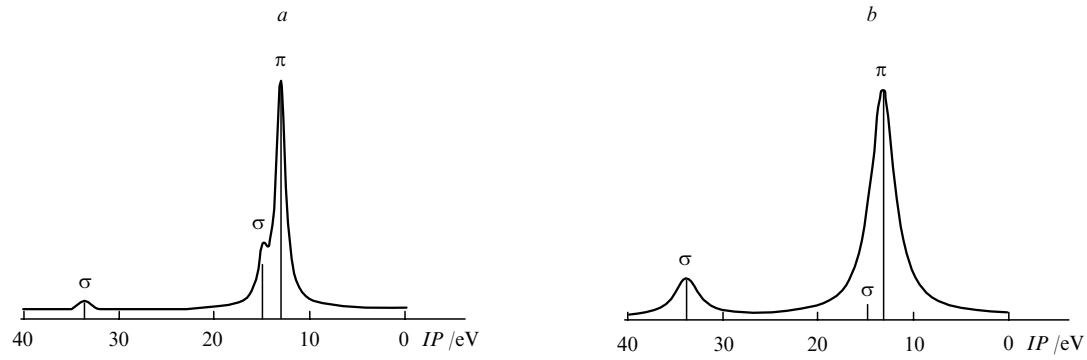


Figure 14. Theoretical X-ray NK_α- (*a*) and BK_α-emission spectra (*b*) of boron nitride (MNDO calculation). The vertical bars show the contributions of atomic N2p (*a*) and B2p orbitals (*b*) to the MO.

nitride spectra (see Refs 37, 158, 167 and 171–180). In fact, for a one-dimensional layer of crystalline hBN (assuming weak interaction between the layers), band electron states can be subdivided according to σ- and π-symmetry corresponding to σ- and π-bonding between atoms. The electric-field vector of the electromagnetic wave (polarisation plane) appearing due to the transition, *e.g.*, from the π-state to a 1s-vacancy, is parallel to the $2p_z$-orbital. If one varies the orientation of the analyser crystal (which expands the emission radiation into a spectrum) relative to the boron nitride single crystal, it is possible to record changes in the intensity of the band related to the π-state and even its disappearance.[42, 171, 172] The use of SI for studying this effect provides yet another advantage. The point is that such radiation becomes plane-polarised. By changing the angle between the incidence radiation and the plane of the boron nitride crystal (grazing incidence angle), one can also observe changes in the intensity of the π-band in the spectrum. The emission spectra of hBN obtained with the use of SI at different grazing incidence angles[37] are presented in Fig. 15.

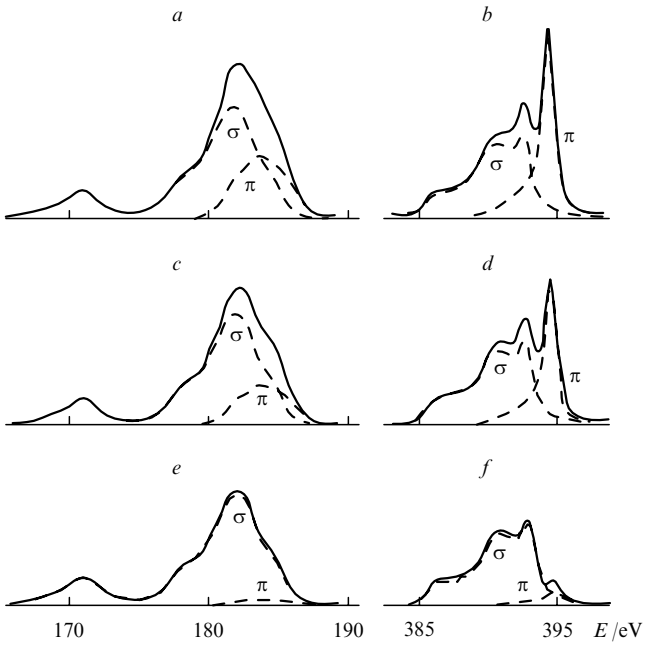


Figure 15. Orientation effects in X-ray BK_α- (*a*, *c*, *e*) and NK_α-emission spectra (*b*, *d*, *f*) of hexagonal boron. Dependence of the relative intensities of the lines corresponding to σ- and π-bonds on the angle between the incident polarised radiation and the crystal surface (grazing incidence angle θ).[37]
$\theta = 10^\circ$ (*a*, *b*), 30° (*c*, *d*), 80° (*e*, *f*).

The X-ray spectra of boron phosphide were studied.[104, 114, 117, 137, 151, 195–197] A comprehensive X-ray spectral study of this compound was carried out; its BK_α-, PK_β- and P$L_{2,3}$-emission spectra, as well as B*K*-, P*K*- and P$L_{2,3}$-absorption spectra were obtained.[104, 151, 195, 196] The dependence of BK_α-spectrum on the excitation radiation length was studied.[137, 197] Interpretation of boron phosphide spectra was carried out.[198] Studies reporting X-ray emission spectra of boron and phosphorus in $B_{13}P_2$ and $B_{13}As_2$ are also of note.[117, 136]

4. Boron halides and their derivatives

X-Ray BK_α- and FK_α-emission spectra of boron trifluoride (D_{3h} symmetry group) in solid [138] and gaseous [199] states were published. Studies of X-ray absorption by BF_3 are more numerous. For example, X-ray B*K*-absorption spectra [104, 115, 129, 200–205] and F*K*-absorption spectra [204–206] were described. In some studies,[201–203, 206] SI was used to obtain X-ray spectra of boron

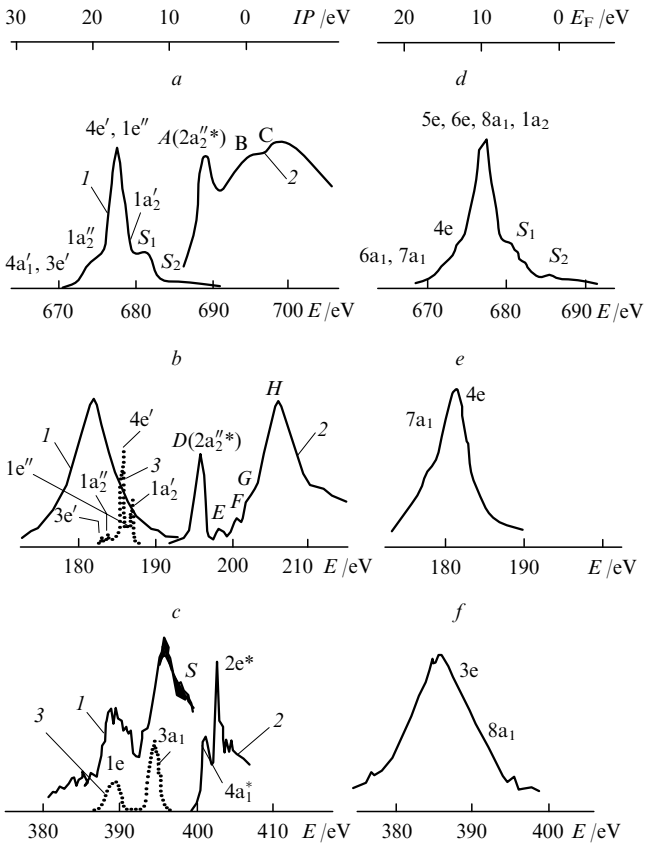


Figure 16. Experimental X-ray and photoelectron [He(I)] spectra of NH_3 and BF_3 (*a*–*c*) and X-ray emission spectra of $NH_3 \cdot BF_3$ (*d*–*f*).
(*a*) FK_α- (*1*) [199] and F*K*-spectra (*2*);[204] (*b*) BK_α- (*1*),[199] B*K*-spectra (*2*) [115] and photoelectron spectrum of BF_3 (*3*);[223] (*c*) NK_α- (*1*),[199] N*K*-spectra (*2*) and photoelectron spectrum of NH_3 (*3*);[227] (*d*) FK_α-spectrum; (*e*) BK_α-spectrum; (*f*) NK_α-spectrum.[199] (*IP* is the ionisation potential relative to the vacuum for the gas phase, E_F is the ionisation potential relative to the Fermi level for the solid phase, *E* is the X-ray transition energy. See the text for the designations of the lines.)

trifluoride. Electron energy loss spectra were recorded for BF_3;[207] moreover, vibration excitation upon inelastic scattering of electrons on this molecule was studied.[208] The spectra of boron trifluoride were also discussed elsewhere.[209–218] Experimental emission spectra were compared with theoretical spectra obtained by *ab initio* calculations on the electronic structure of BF_3.[199] The X-ray BK_α-emission spectrum of BF_3 was calculated by the Xα-DV method.[122] X-Ray absorption spectra of the BF_3 molecule were analysed by quantum-chemical methods.[219–222] The X-ray emission BK_α- and FK_α-spectra of boron trifluoride [199] are presented in Fig. 16*a*. It also shows the X-ray B*K*- and F*K*-absorption spectra [115, 204] and the photoelectron spectrum of boron trifluoride.[223] (XPS data for BF_3 were taken from Ref. 224.) Figure 17 presents theoretical X-ray emission spectra.[199] In the boron trifluoride molecule, the $2a_2''$ π-type orbital acts as the LUMO. This vacant (acceptor) orbital interacts with the orbital of the lone electron pair of the donor molecule resulting in the formation of a donor–acceptor bond. This orbital manifests itself as rather distinct lines *A* and *D* in X-ray B*K*- and F*K*-absorption spectra (see Fig. 16*a*,*b*). The interpretation of other lines in B*K*- and F*K*-spectra (*B*, *C*, *E*, *F*, *G* and *H*) and the dissention that appeared in this connection were discussed.[207, 208] The assignment of lines in the X-ray emission spectra of boron trifluoride (occupied orbitals) is demonstrated in Fig. 16. Studies showed that the MOs whose electron density is located on fluorine atoms are the highest occupied orbitals. They are followed by MOs with predominant population on the boron atom. The *S*, S_1 and S_2

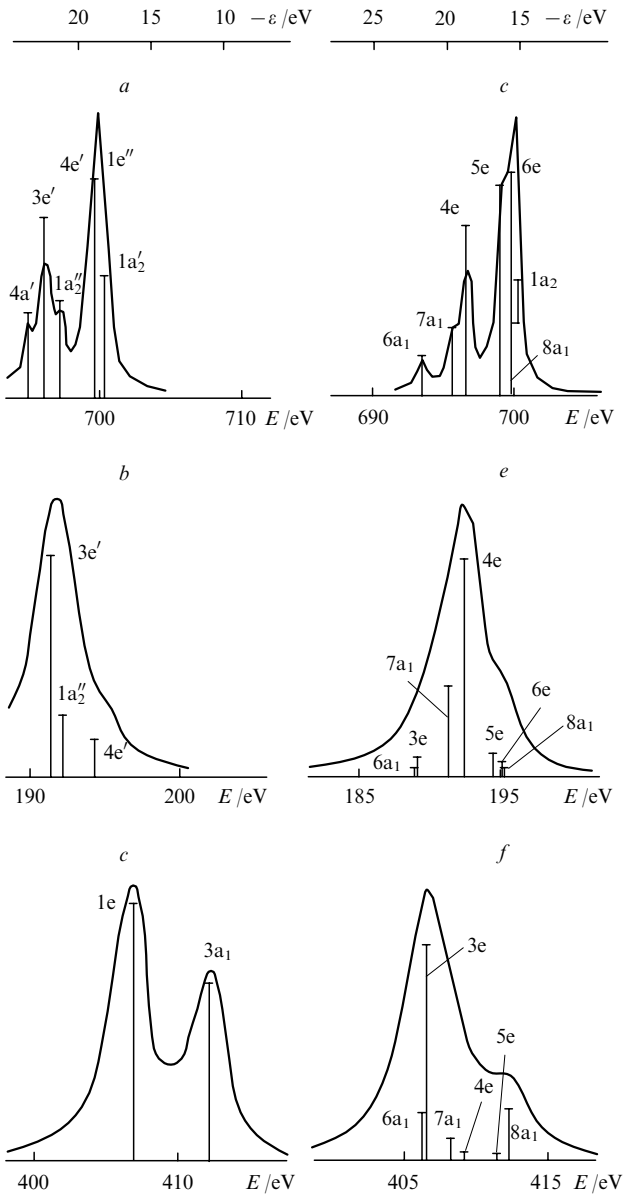


Figure 17. Theoretical X-ray emission spectra of NH_3 and BF_3 (*a*–*c*) and $NH_3 \cdot BF_3$ (*d*–*f*) obtained by *ab initio* calculations.[199]
(*a*, *d*) FK_α-spectra; (*b*, *e*) BK_α-spectra; (*c*, *f*) NK_α-spectra (ε is orbital energy). The vertical bars show the contributions of atomic orbitals to the MOs.

maxima are caused by electron transitions in double-ionised molecules; they are generally not considered in interpretations of X-ray spectra in the context of chemical bond studies (see, *e.g.*, Ref. 99).

Boron trichloride has only been studied by X-ray absorption spectroscopy. The X-ray B*K*- and Cl$L_{2,3}$-absorption spectra of BCl_3 [104, 200, 202, 218, 225, 226] almost coincide. The spectra were interpreted based on *ab initio* [202] and CNDO/2 [219] calculations. Identification of separate lines in the X-ray absorption spectrum of boron trichloride was reported.[225, 226] It was noted [200] that the B*K*-absorption spectrum of BCl_3 is less shifted towards high energies than the similar spectrum of BF_3. This results from the fact that the effective positive charge on the B atom in boron trichloride is lower. The X-ray B*K*-absorption spectrum of BBr_3 was obtained and its interpretation based on *ab initio* calculations was carried out.[202]

Let us consider in more detail the $NH_3 \cdot BF_3$ complex (symmetry group C_{3v}), which is formed upon donor–acceptor interaction of NH_3 and BF_3 molecules. This complex was studied by X-ray spectral methods.[199] The ammonia and boron trifluoride molecules were first considered separately, then changes observed in the spectra during complexing were noted. The experimental and theoretical X-ray spectra [199] and the photoelectron spectra of ammonia [227] and boron trifluoride [223] are shown in Figs 16 and 17. The spectra were compared using the energy positions of inner-shell electrons.[224] The absorption spectrum of $NH_3 \cdot BF_3$ was obtained by Akimov *et al.*[228] The spectrum structure was identified using calculations in the *ab initio* and MNDO approximations.[199]

The scheme of MOs of ammonia, boron trifluoride and the $NH_3 \cdot BF_3$ complex composed using the results of MNDO calculations [199] is shown in Fig. 18. It also presents results of fragment analysis (expansion of a molecule's MOs into the constituent fragment orbitals).[229] It should be expected within the framework of donor–acceptor bonding that the main interacting orbitals include the $3a_1$ HOMO of ammonia and the $2a_2''^*$ LUMO of boron trifluoride (or $6a_1^*$ in pyramidal configuration, symmetry group C_{3v}, for BF_3 in the complex with ammonia). It is evident from Figs 16–18 that these are orbitals ($3a_1$ and $2a_2''^*$) with high contributions of the 2p-AOs of nitrogen and boron, respectively. It follows from calculations (see Fig. 18) that the nitrogen–boron bond in $NH_3 \cdot BF_3$ mainly involves electrons of three MOs, *viz.*, $8a_1$, $7a_1$ and $6a_1$; the properties of the wave functions of remaining occupied MOs are similar to those of the original molecules (NH_3 and BF_3). Orbitals with a_1 symmetry are bonding and appear due to interaction of the $3a_1$-MO of ammonia with $6a_1^*$-, $5a_1$- and $4a_1$-MOs of boron trifluoride. It should be noted that only the formation of the $8a_1$ orbital predominantly involves the vacant $6a_1^*$-MO of boron trifluoride (see Fig. 18). Hence, the $8a_1$-MO can be related (to a certain approximation) to the bonding orbital of

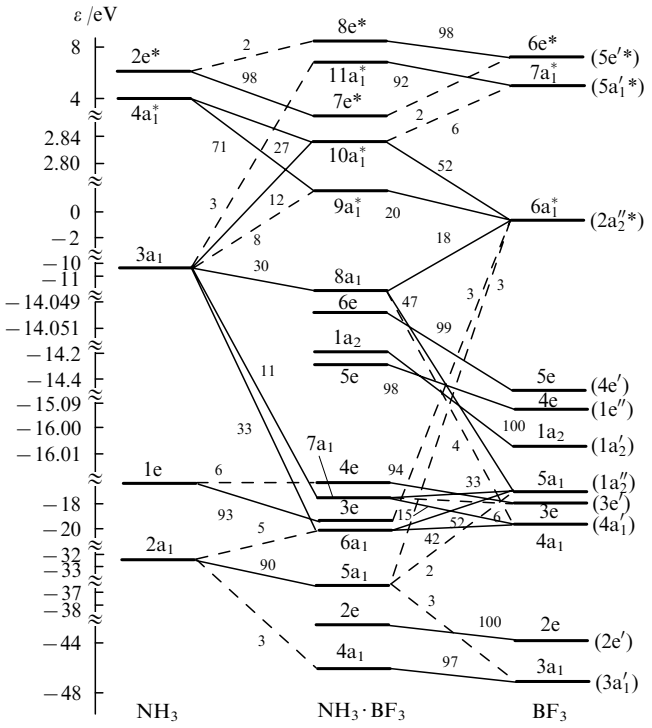


Figure 18. Correlation diagram of MOs for the $NH_3 \cdot BF_3$ complex and its fragments, NH_3 and BF_3. Results of MNDO calculation.[199]
The calculation was carried out for the pyramidal BF_3 molecule (C_{3v} symmetry); designations of the corresponding MO of the planar BF_3 molecule (D_{3h} symmetry) are given in parentheses. The numbers near the connecting lines correspond to the contributions (in percent) of the orbitals of the NH_3 and BF_3 fragments to the MOs of the $NH_3 \cdot BF_3$ molecule. Dashed lines indicate contributions smaller than 10%.

the two-level donor–acceptor bond model (see Section III.2), though it involves rather a large contribution (~47%) of the occupied $5a_1$ orbital of the acceptor. The changes in the electronic structure on passage from isolated NH_3 and BF_3 molecules to the $NH_3 \cdot BF_3$ complex are reflected in X-ray NK_α-emission spectra (see Figs 16 and 17). The intensity ratio of lines $I(8a_1)/I(3e)$ in the spectrum of the complex is much lower than the $I(3a_1)/I(1e)$ ratio in the spectrum of pure NH_3. Since it follows from calculations that the 1e-MO of ammonia and the 3e-MO of the $NH_3 \cdot BF_3$ complex are similar, the relative intensities of their corresponding X-ray lines almost do not change, hence one can state that the contribution of the N2p-AO to the $8a_1$ HOMO of the complex is smaller than that of the similar $3a_1$-MO of ammonia. This can serve as a confirmation of electron density transfer from the ammonia molecule to the boron trifluoride molecule, which mainly involves the highest valence MOs. The complex in question contains two vacant orbitals, *viz*., $9a_1^*$ and $10a_1^*$ (see Fig. 18), which can be matched with the vacant MO in the two-level model (see Section III.2). Data of experimental and theoretical studies [199] of the $NH_3 \cdot BF_3$ complex (see Figs 16–18) allow the character of electron density distribution in it to be understood. For example, the highest occupied orbitals are mainly populated by F2p electrons. At higher binding energies, predominant contribution to the orbitals is made by boron 2p-AOs. The deepest valence MOs are mostly composed of nitrogen 2p-AOs. It should also be noted that the overlapping of bands in the NK_α- and BK_α-spectra evident when they are compared can suggest that the nature of the B–N bond is largely covalent.

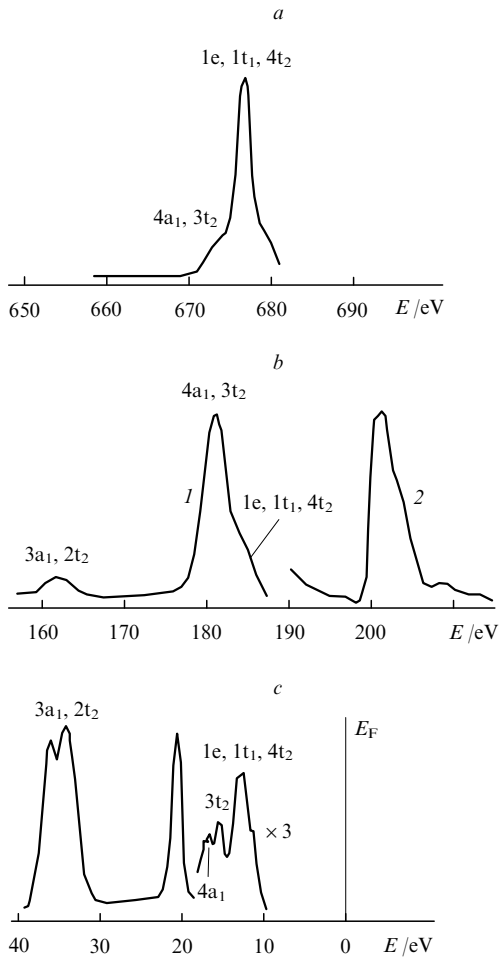


Figure 19. X-Ray emission FK_α- (*a*) and BK_α-spectra (*b*, spectrum *1*),[231] B*K*-absorption spectrum (*b*, spectrum *2*)[128] and X-ray photoelectron spectrum in the valence band of BF_4^- (*c*).[231]

X-Ray emission spectra of boron and fluorine were obtained for $BF_3 \cdot C_6H_5CH{=}NC_6H_4Me\text{-}p$.[138]

Compounds KBF_4 and NH_4BF_4 (the point symmetry group of the BF_4^- anion is T_d) were studied by X-ray emission spectroscopy, and K_α-emission spectra of boron [230,231] and fluorine [231] were obtained. X-Ray B*K*-absorption spectra were studied [128,129] using SI as the excitation source. Figure 19 presents X-ray emission spectra and X-ray photoelectron spectra in the valence band for the BF_4^- anion [231] and its X-ray absorption spectra.[128] Identification of spectral lines was carried out elsewhere.[231]

5. Boron hydrides and their derivatives

a. Simplest systems

Experimental X-ray spectral data for borane (BH_3) are unavailable. This results from the fact that BH_3 molecules do not exist as monomers under ordinary conditions; they occur as B_2H_6 bridge dimers (see Fig. 5*e*). The X-ray absorption spectrum of diborane was obtained by Zimkina and Vinogradov.[204]

Analysis of the electronic structure of $Me_3N \cdot BH_3$ based on X-ray emission spectroscopy data was carried out.[230] X-Ray BK_α- and NK_α-emission spectra were obtained. A comparison of X-ray NK_α-emission spectra of Me_3N and its adduct with BH_3 showed that the relative intensity of the line in the X-ray emission spectrum of trimethylamine associated with the lone electron pair decreases abruptly in the $Me_3N \cdot BH_3$ spectrum.[230,232] As with the $NH_3 \cdot BF_3$ complex discussed above (see Section IV.4), this results from electron density transfer from the trimethylamine nitrogen atom to the vacant orbital of the borane molecule with formation of a donor–acceptor bond.

The anions BH_4^- with tetrahedral symmetry in the KBH_4 and $NaBH_4$ molecules were studied;[230] X-ray emission [230] and absorption [128] spectra were obtained.

b. $B_nH_n^{2-}$ anions and boron clusters

The *closo*-borane anions $B_{10}H_{10}^{2-}$ and $B_{12}H_{12}^{2-}$ (symmetry groups D_{4d} and I_h, respectively, see Fig. 6*a*), the electronic structures of which were studied by X-ray spectroscopy,[230,233] are characterised by considerable electron density delocalisation over the entire cluster, which determines their aromatic properties and unusually high resistance to decomposition in different chemical reactions (see the references in Ref. 230). The geometric structure of the $B_{10}H_{10}^{2-}$ anion is such (see Fig. 6*a*) that two groups of equivalent boron atoms exist, *viz*., vertex atoms B(1) and B(10) and equatorial atoms (all the rest). Their coordination numbers are 5 and 6, respectively; a greater negative charge is localised on atoms with the smaller coordination number, *i.e*., B(1) and B(10), in the cluster.[230,233]

Figure 20 demonstrates the X-ray BK_α- and Cu$L_{\alpha1,2}$-emission spectra of $Cu_2B_{10}H_{10}$ and the X-ray BK_α-emission spectrum of $Cs_2B_{10}H_{10}$. These spectra show that the distribution maximum of copper 3d-electron density is located in the upper part of the valence band (~3.3 eV below the Fermi level), whereas the distribution maximum of boron 2p-electron density corresponds to its lower part (~6.7 eV below the Fermi level). The observed overlapping of the BK_α- and Cu$L_{\alpha1,2}$-bands allows one to assume that the interaction of the copper 3d-orbitals with the hydroborate anion is of covalent nature.[230,233]

The shape of the BK_α-emission spectrum of ionic $Cs_2B_{10}H_{10}$ and the energy positions of lines in it (Fig. 20) remain almost unchanged, which results most likely from delocalisation of valence electrons in the $B_{10}H_{10}^{2-}$ anion stabilising the system of its valence MOs.

X-Ray emission BK_α- and CK_α-spectra of *ortho*- and *meta*-carboranes(12) 1,2- and 1,7-$C_2B_{10}H_{12}$ were studied [234] (see Fig. 5*g*,*h*); the electronic structures of these compounds were calculated by the *ab initio* method in the 6-31G* basis set and the corresponding simulated spectra were obtained (Fig. 21). Correlation and fragment analysis of the MOs of these compounds and the $B_{12}H_{12}^{2-}$ boron cluster were carried out (Fig. 22).

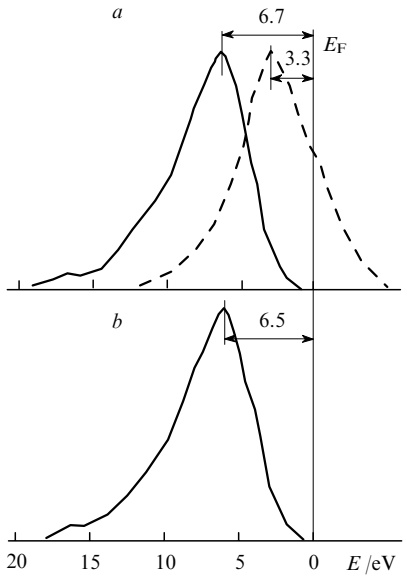


Figure 20. X-Ray emission BK_α-spectra (solid lines) of $Cu_2B_{10}H_{10}$ (*a*) and $Cs_2B_{10}H_{10}$ (*b*).[230]
The dashed line shows the X-ray Cu$L_{\alpha 1,2}$ emission spectrum.

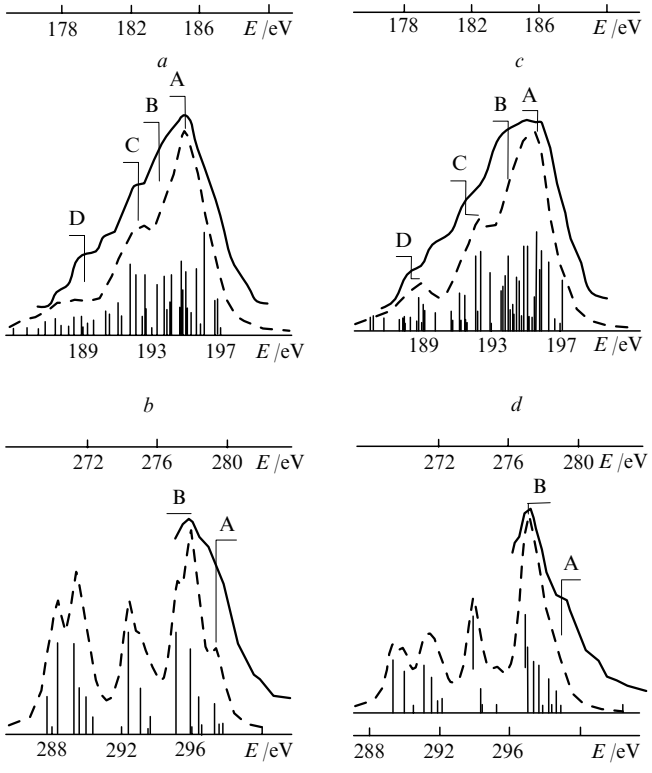


Figure 21. Experimental (solid lines, upper scales of transition energies) and theoretical (dashed lines, lower scales) X-ray emission spectra of 1,2-$C_2B_{10}H_{12}$ (*a*, *b*) and 1,7-$C_2B_{10}H_{12}$ (*c*, *d*).[234]
(*a*, *c*) BK_α-spectra; (*b*, *d*) CK_α-spectra.

Electron energy loss spectra (see Section III.2) were obtained for a series of boranes and carboranes, *viz*., *nido*-pentaborane(9) (B_5H_9), *nido*-2,3-diethyl-2,3-dicarbahexaborane(8) ($Et_2C_2B_4H_6$), *nido*-decaborane(14) ($B_{10}H_{14}$), *closo-o*-carborane ($C_2B_{10}H_{12}$), and 1,2-dicarbaundecaborane(11) ($C_2B_9H_{11}$).[235, 236] Quantum-chemical calculations of the electronic structures of these compounds

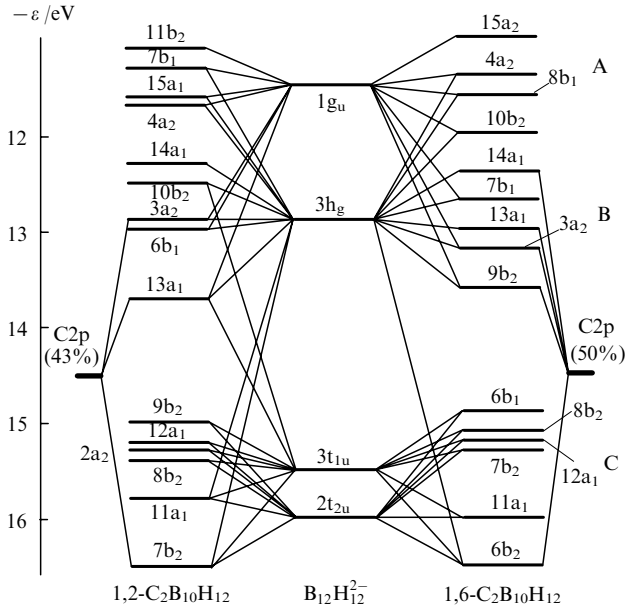


Figure 22. Correlation diagram (MNDO calculation) of energy levels in the $B_{12}H_{12}^{2-}$ anion, 1,2-$C_2B_{10}H_{12}$ and 1,7-$C_2B_{10}H_{12}$.[234]
The capital letters A, B and C designate the MOs which appear as the corresponding maxima in the X-ray spectra; the numbers in parentheses indicate the total contributions of the carbon 2p-AOs to the MOs.

were carried out in the MNDO and EHMO approximations (extended Hückel method); this served as a basis for composing theoretical spectra and interpreting experimental spectra.[235, 236]

c. Borane clusters with Lewis bases ($B_{10}H_{12}L_2$)

The electronic structure of borane clusters $B_{10}H_{12}L_2$ (where L is a Lewis base) was considered in terms of X-ray emission transitions for three compounds, *viz*., $B_{10}H_{12}(NH_3)_2$, $B_{10}H_{12}(SMe_2)_2$ and $B_{10}H_{12}(PPh_3)_2$.

X-Ray studies of 6,9-bis(ammonia)-*arachno*-decaborane(12) [$B_{10}H_{12}(NH_3)_2$] have been carried out.[230, 237, 238] The structure of this cluster (point symmetry group C_{2v}) and the atom numbering in it are shown in Fig. 6*d*. When considering the electronic structure of $B_{10}H_{12}(NH_3)_2$ it was assumed that its molecule consists of two fragments, *viz*., the borane cluster ($B_{10}H_{12}$) and the ammonia molecule.[237, 238] The chemical bond between these fragments is assumed to be of donor–acceptor nature; the NH_3 molecule acts as a donor, while the borane fragment is an acceptor. Quantum-chemical calculations of the electronic structure of the $B_{10}H_{12}(NH_3)_2$ cluster and its fragments, *i.e*., $B_{10}H_{12}$ and NH_3, were carried out using the MNDO method.[238, 239] Figure 23*a* shows the correlation diagram built on this basis and the results of fragment analysis of the composition of the $B_{10}H_{12}(NH_3)_2$ molecular orbitals formed by the MOs of the fragments, *i.e*., the $B_{10}H_{12}$ borane cluster and the NH_3 molecule. Among the highest occupied orbitals of the $B_{10}H_{12}$ cluster, one can note a group of MOs, *e.g*., $3a_2$, $8a_1$ and $5b_1$, which become orbitals of the complex and almost do not change their symmetry upon coordination of ammonia. In this case, they are shifted upwards in parallel with a decrease in the binding energy (see Fig. 23*a*). Similar behaviour is observed for deeper MOs. For example, the $5b_2$ orbital of the $B_{10}H_{12}$ cluster contributes noticeably to the $8b_2$-MO of the complex. The electrons of this orbital are localised in the cluster and are not involved in the formation of the chemical bond with ammonia. The formation of the orbitals of the complex responsible for the interaction of ammonia with the borane fragment involves not only the vacant MOs of the $B_{10}H_{12}$ cluster as an acceptor but also its occupied orbitals, which play an important role in the process. While only electrons of the $3a_1$

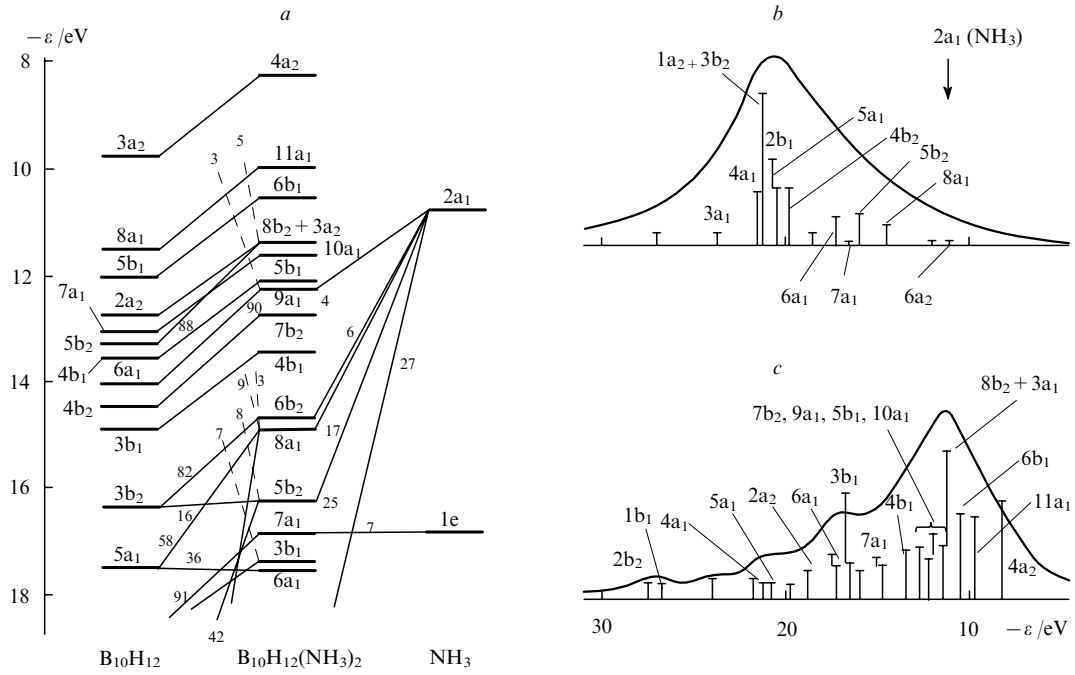


Figure 23. Energies of MOs of the $B_{10}H_{12}(NH_3)_2$ fragments (*a*) and theoretical NK_α- (*b*) and BK_α-spectra (*c*) of $B_{10}H_{12}(NH_3)_2$.[238]
The numbering is only given for valence orbitals. If only one orbital of a fragment contributes to a MO of $B_{10}H_{12}(NH_3)_2$ and this contribution is above 95%, then its value is omitted; dashed lines indicate the contributions of the vacant orbitals of $B_{10}H_{12}$. The vertical bars show the contributions of atomic orbitals to the MOs.

orbital of the ammonia molecule ($2a_1$ if only valence orbitals are numbered, see Fig. 23 *a*) interact with the borane cluster, several vacant orbitals rather than one orbital of the borane fragment are involved in the interaction. Although their contributions to each MO of the complex, including deep orbitals with ionisation potentials ~16–17 eV, are insignificant and amount to several percent (as shown by numbers near the dashed lines in Fig. 23 *a*), their total contribution is ~30%. The theoretical X-ray NK_α- and BK_α-spectra built on the basis of MNDO calculations are presented in Fig. 23 *b*,*c*, respectively.

The experimental X-ray emission spectra of $B_{10}H_{12}(NH_3)_2$ are presented in Fig. 24.[238] For comparison, the X-ray spectrum of ammonia is also shown. The $B_{10}H_{12}$ fragment does not exist in a free state, and it is worthwhile to compare its X-ray BK_α-emission spectrum with a spectrum of some boron cluster with similar electronic structure, *e.g.*, $B_{10}H_{14}^{2-}$. Yumatov *et al.*[238] used $Cs_2B_{10}H_{10}$ for such a comparison. Although its electronic structure differs from that of the cluster fragment in question ($B_{10}H_{12}$), the X-ray BK_α-emission spectra of $Cs_2B_{10}H_{10}$ and $B_{10}H_{12}(NH_3)_2$ almost coincide (see Fig. 24 *b*,*d*). This suggests that X-ray BK_α-spectra provide little information in studies of borane clusters. It is likely that X-ray spectral equipment with higher resolution is required to improve this method.

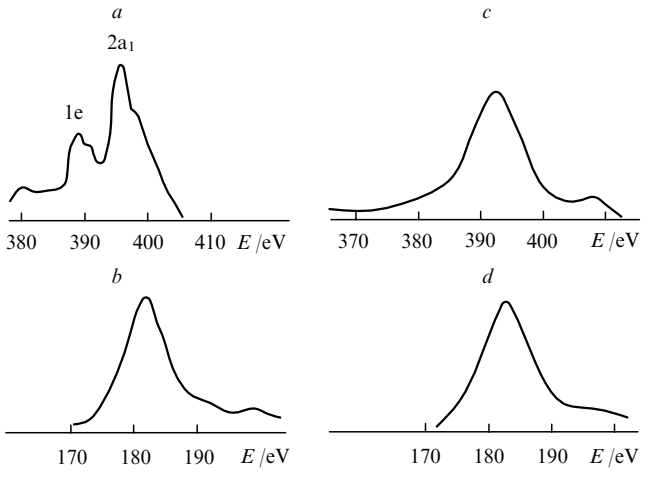


Figure 24. Experimental X-ray NK_α-emission spectra of ammonia (*a*) and BK_α-spectra of $Cs_2B_{10}H_{10}$ (*b*); NK_α- (*c*) and BK_α-spectra (*d*) of the $B_{10}H_{12}(NH_3)_2$ complex.[238]
All the spectra are smoothed.

A characteristic feature of changes in the X-ray NK_α-emission spectrum on transition from the NH_3 molecule to the $B_{10}H_{12}(NH_3)_2$ cluster (see Fig. 24 *a*,*c*) is that the relative intensity of the high-energy band ($2a_1$-MO of ammonia) decreases; as shown for the $NH_3 \cdot BF_3$ cluster (see Section IV.4), this is due to electron density transfer from the nitrogen atom to the boron atom. Since the X-ray BK_α-emission spectrum of $B_{10}H_{12}(NH_3)_2$ is shifted towards lower binding energies (or towards higher electron transition energies) with respect to the NK_α-spectrum more strongly, it can be concluded that the highest occupied orbitals of this compound include those MOs whose electron density is mainly localised on the borane cluster atoms. This feature of electron density distribution also follows from results of quantum-chemical calculations [238, 239] (see Fig. 23). The main parameters of X-ray spectra built on the basis of calculated data agree with the corresponding characteristics of the experimental spectra. Thus, the results of the X-ray spectral study on the formation of chemical bonds between ammonia and borane cluster in the $B_{10}H_{12}(NH_3)_2$ complex allow the conclusion to be drawn that this process is accompanied by electron density transfer from NH_3 to $B_{10}H_{12}$ (see Refs 230, 237 and 238). The results of analysis performed on the basis of quantum-chemical calculations [238, 239] also confirm that electron density on the nitrogen atom decreases and on the B(6) and B(9) atoms involved in the coordination increases (see Fig. 6 *c*).

X-Ray studies of 6,9-bis(dimethyl sulfide)-*arachno*-decaborane(12) [$B_{10}H_{12}(SMe_2)_2$] were carried out by Murakhtanov *et al.*[239] and by Yumatov *et al.*[240] Figure 25 shows a correlation

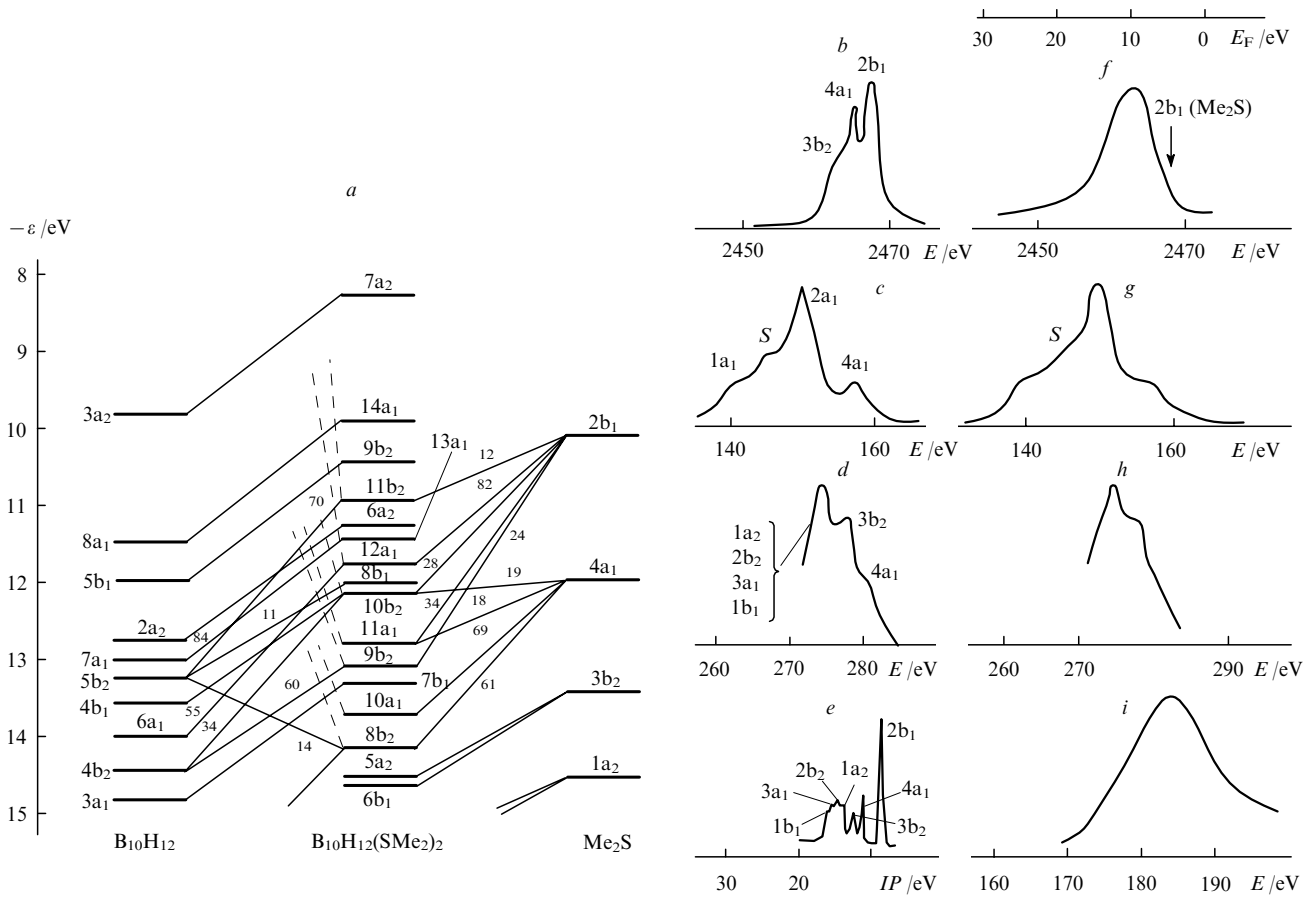


Figure 25. Scheme of MOs of the $B_{10}H_{12}(SMe_2)_2$ cluster and its fragments (*a*), experimental X-ray and UV [He(I)] photoelectron spectra of Me_2S (*b*–*e*) and experimental X-ray spectra of $B_{10}H_{12}(SMe_2)_2$ (*f*–*i*).[240]
(*b*,*f*) SK_β-spectra; (*c*, *g*) S$L_{1,2}$-spectra; (*d*, *h*) CK_α-spectra, (*e*) UPS spectrum; (*i*) BK_α-spectrum. Dashed lines indicate the contributions of vacant orbitals.

diagram of MOs of the $B_{10}H_{12}(SMe_2)_2$ cluster and of its fragments ($B_{10}H_{12}$ and Me_2S); the results of fragment analysis of this cluster (MNDO calculation); the X-ray and UV [He(I)] [227] photoelectron spectra of Me_2S reduced to a common energy scale (with the use of XPS data [224]); and X-ray spectra of $B_{10}H_{12}(SMe_2)_2$. The point symmetry group of both compounds is C_{2v}. As one can see from Fig. 25 *b*,*f*, the most noticeable changes on transition from dimethyl sulfide to its adduct with borane are observed in the X-ray SK_β-emission spectrum. They are similar to the changes observed in X-ray spectra upon coordination of the ammonia molecule to the borane cluster. The maxima in all emission spectra of free dimethyl sulfide are also identified in this figure.[96, 241] For example, the $2b_1$ HOMO is formed by a lone electron pair or, more accurately, it is an orbital with high S3p-population. Interaction of the $2b_1$ HOMO of Me_2S with the $5b_2$, $6a_1$ and $4b_2$ orbitals of $B_{10}H_{12}$ upon coordination of a dimethyl sulfide molecule to the borane cluster (see Fig. 25 *a*) results in a series of new MOs, *viz*., $11b_2$, $12a_1$, $10b_2$ and $11b_2$ (see Fig. 25 *a*); the contribution of the 3p-AO of the sulfur atom to these orbitals is much lower than the contribution to the $2b_1$ HOMO of the free dimethyl sulfide molecule. Hence, the X-ray SK_β-emission spectrum will contain a low intensity line instead of the intense line corresponding to the lone electron pair (see Fig. 25 *b*,*f*). On the other hand, the structure of deeper MOs changes insignificantly. Thus, it can be concluded that the chemical bond between dimethyl sulfide and the borane cluster is of donor–acceptor nature and that it is formed by the lone electron pair of Me_2S and the 2p-orbitals of boron. The correlation diagram shows that the structure of the wave functions of the three occupied MOs, *viz*., $7a_2$, $14a_1$ and $9b_1$, of the $B_{10}H_{12}(SMe_2)_2$ cluster almost coincides with the structure of the three orbitals of the borane cluster in a free state (see Fig. 25 *a*). The only difference is that the bond energy in the $B_{10}H_{12}(SMe_2)_2$ cluster is lower. The electron densities of the MOs of the above adduct are localised on boron atoms (and are absent from the ligands). This electron density distribution is clearly seen in the X-ray spectra. In fact, as one can see in Fig. 25 *f*–*i*, as the binding energy increases, the boron line with a maximum at ~5 eV with respect to the Fermi level (transition energy ~184 eV) characterising the contributions of the boron 2p-AO to the MO is the first line to appear; it is followed by lines characterising the contributions from the AOs of the ligands starting from the first line of the S$L_{2,3}$-spectrum with a maximum of ~7 eV with respect to the Fermi level. It can be concluded from a comparison of spectra arranged in this way that the electron density of the highest MOs is predominantly localised on borane cluster atoms. In the dimethyl sulfide molecule, lone electron pairs ($2b_1$-MO) are involved actively in the chemical bond with the borane cluster, including the B(6) and B(9) atoms (see Fig. 6 *c*). It was shown [240] that in this case one can speak of preferential formation of an S–B donor–acceptor σ-bond. Finally, deeper MOs of the borane–Me_2S adduct are mainly composed of dimethyl sulfide's MOs. The formation of the chemical bond between the borane cluster and dimethyl sulfide molecules with involvement of vacant orbitals has certain specific features. Their contribution is spread along the series of the $B_{10}H_{12}(SMe_2)_2$ MOs and does not exceed 8% for any single orbital, although the total contribution of the vacant boron 2p-AOs amounts to 30%. The same situation is observed for the $B_{10}H_{12}(NH_3)_2$ cluster. It follows from quantum-chemical studies (MNDO calculations) [239] that a bond of predominantly σ-type is formed between the B(6), B(9) and L atoms (see Fig. 6 *d*). However, a contribution of the π-component is also possible in

some cases, *e.g.*, with L = MeCN and C_2H_5N. This interaction is very weak in the $B_{10}H_{12}(NH_3)_2$ cluster.

Changes in the valence of a sulfur atom with different coordinations on transition from such non-cluster compounds as H_2S and Me_2S (with a coordination number of 2) to $B_{10}H_{12}(SMe_2)_2$ and, finally, to the $B_9SH_{12}^-$ anion, in which the sulfur atom is directly introduced in the borane cluster,[240] with a coordination number of 3, were studied. The changes in the chemical bond nature between the sulfur and boron atoms on passing from the $B_{10}H_{12}(SMe_2)_2$ cluster to the $B_9SH_{12}^-$ anion are no less interesting. The geometric structure of this anion and its X-ray SK_β-emission spectrum obtained by Yumatov *et al.*[240] are presented in Fig. 26. The sulfur atom in the H_2S molecule forms two σ-bonds with hydrogen atoms, whereas the dimethyl sulfide molecule contains two similar S–C σ-bonds along with a weak π-bond resulting from interaction of a lone electron pair of the sulfur atom with the 2p-electrons of the carbon atoms. This interaction does not affect considerably the structure of the X-ray SK_β-emission spectrum on transition from H_2S to Me_2S (see Figs 25 and 26): just a small decrease of the relative intensity of the line corresponding to the lone electron pair of the sulfur atom (b_1-MO) is observed. As noted previously, the sulfur atom in the $B_{10}H_{12}(SMe_2)_2$ molecule forms a σ-type chemical bond (donor–acceptor bond) with a boron atom and two σ-bonds with carbon atoms of the methyl groups. In the $B_9SH_{12}^-$ thiaborane cluster (see Fig. 26), the sulfur atom forms two σ-bonds with the B(5) and B(7) atoms. By analogy with the dimethyl sulfide molecule, one can assume that there is weak π-interaction between these sulfur and boron atoms. The conjugation of the S atom with the B(2) cluster atom possibly involves a lone electron pair of the sulfur atom. Similar interaction manifests itself in X-ray SK_β-emission spectra on transition from the Me_2S molecule to the $B_{10}H_{12}(SMe_2)_2$ cluster. The line in the X-ray SK_β-emission spectrum of CsB_9SH_{12}, which was associated with a lone electron pair on the sulfur atoms in the spectra of H_2S and Me_2S (see Fig. 26), has very low intensity. The identity of X-ray SK_β-emission spectra of $B_{10}H_{12}(SMe_2)_2$ and CsB_9SH_{12} confirms the assumption that the electronic states of the sulfur atom coordinated by three boron atoms in these clusters are similar. Hence, it can be assumed that noticeable conjugation of the lone electron pair of the sulfur atom with the 2p-electrons of the boron atoms occurs in the CsB_9SH_{12} cluster, but it appears impossible to determine the type of the S–B(2) interaction based on X-ray spectral data only. Most likely, mixing of σ- and π-bonding occurs in this case, and it is the reason for the strong decrease in the electron-donor properties of the sulfur atom incorporated in the borane cluster.

Thus, the S–B chemical bond in $B_{10}H_{12}(SMe_2)_2$ results from σ-interaction of the HOMO of dimethyl sulfide, which predominantly consists of the 3p-AO of the sulfur atom (lone electron pair), with orbitals of the borane cluster. The interaction of similar orbitals of B and S atoms probably occurs in the CsB_9SH_{12} molecule as well. The results considered above reflect the substantial differences in the electronic state of sulfur atoms in non-cluster systems and in borane clusters with various coordination numbers. These differences can manifest themselves as differences in the reactivity of the systems in question.

Interaction of a ligand with the borane cluster in the molecule $B_{10}H_{12}(PPh_3)_2$ is no less complex.[242] The point is that the lone electron pair of the phosphorus atom in the free triphenylphosphine molecule interacts with electrons of the phenyl groups.[110, 241] This affects markedly the structure of the X-ray PK_β-emission spectrum (Fig. 27). In fact, transition from triethylphosphine, in which this kind of interaction is absent, to triphenylphosphine is accompanied by a decrease in the relative intensity of the high-energy line caused by the lone electron pair of the phosphorus atom. One would think that the addition of a Ph_3P molecule to the $B_{10}H_{12}$ borane cluster would decrease the relative intensity of this line even more, as it was observed in the X-ray NK_α-emission spectrum on transition from NH_3 to $B_{10}H_{12}(NH_3)_2$ and in the SK_β-spectrum on transition from Me_2S to $B_{10}H_{12}(SMe_2)_2$. However, such an effect is not observed in this case. Possibly, the AO of the lone electron pair of the phosphorus atom in the complex is strongly bound to the MO of the borane cluster and cannot participate in π-conjugation with benzene rings.[242]

In this review, XPS results are considered only in combination with data from X-ray spectroscopy, although the former method is of great value on its own. In particular, this allows one to determine the charge characteristics of atoms in a molecule.[92, 100] Let us provide a few examples. As noted above in the discussion of the X-ray absorption spectra of BF_3 and BCl_3, the electron density on the boron atom is higher in the boron trichloride molecule than

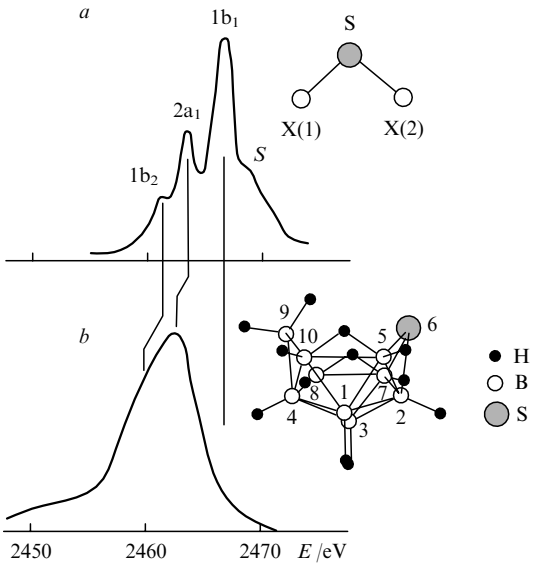


Figure 26. X-Ray SK_β emission spectra of H_2S (*a*) and $B_9SH_2^-$ (*b*) and geometric structure of X_2S (*a*) and $B_9SH_{12}^-$ molecules (*b*).[240]
X = H, Me; *S* is a satellite peak.

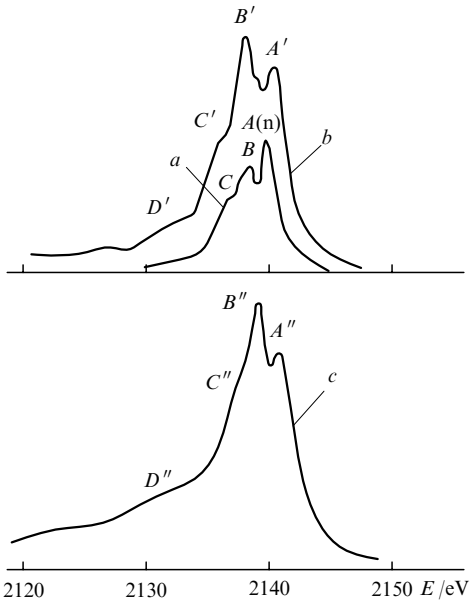


Figure 27. X-Ray PK_β emission spectra of Et_3P (*a*), Ph_3P (*b*) and $B_{10}H_{12}(PPh_3)_2$ (*c*).[242]
Matching spectral lines are designated by the same letters ('n' indicates a lone electron pair).

in the boron trifluoride molecule. According to XPS data, the energy of the B1s level decreases from 202.8 to 200.5 eV on transition from BF_3 to BCl_3 (mean values out of the values available in the database).[224] This also suggests that the electron density on the boron atom is higher in the BCl_3 molecule than in BF_3.[92] The donor–acceptor interaction in $NH_3 \cdot BF_3$ and $B_{10}H_{12}L_2$ (L = NH_3, Me_2S) is accompanied by electron density transfer from the donor molecule to the acceptor molecule. Naturally, this decreases the electron density on the donor atom involved in the coordination. For example, transition from NH_3 to $NH_3 \cdot BF_3$ changes the energy of the N1s level from 398.8 to 402.1 eV,[100] suggesting an increase in the positive charge on the nitrogen atom.[92] Similar behaviour is observed on passage from NH_3 to $B_{10}H_{12}(NH_3)_2$: the energy of the N1s level increases from 398.8 (see Ref. 100) to 402.4 eV,[230] while transition from Me_2S to $B_{10}H_{12}(SMe_2)_2$ changes the energy of the S2$p_{3/2}$-level from 163.0 (see Ref. 100) to 164.4 eV.[243] In these cases, a positive charge also appears on the donor atom involved in the coordination upon the formation of $B_{10}H_{12}(SMe_2)_2$. More detailed XPS studies of boron-containing compounds are covered by reviews.[244, 245]

d. Metalloborane and metallocarborane derivatives

X-Ray spectral studies of Fe^{III}, Co^{III}, Ni^{III} and Ni^{IV} dicarbollyl 'sandwich' complexes were carried out.[230, 246] These compounds include anionic complexes $[M(B_9C_2H_{11})_2]^-$ (M = Fe^{III}, Co^{III}, Ni^{III}) and a molecular complex $[Ni^{IV}(B_9C_2H_{11})_2]^0$. Their ligands include cluster anionic derivatives of *ortho*-carborane(12), $(B_9C_2H_{11})^{2-}$ (see Fig. 6 *j–l*). The M atom in such compounds is located between pentagonal planes $-B-C-C-B-B-$ formed by two $(B_9C_2H_{11})^{2-}$ anions; a 'sandwich' structure is formed as a result. In $[M(B_9C_2H_{11})_2]^{2-}$ complexes, the $-C-C-$ atom pairs in conjugated π-ligands $(B_9C_2H_{11})^{2-}$ can be located *trans* to the M^{III} atom for M = Ni, Fe, *etc*. (see Fig. 6 *j*) or *cis* for M = Co^{III}, as in the $[Ni^{IV}(B_9C_2H_{11})_2]^0$ structure (see Fig. 6 *k*, rotational isomerism). The configuration of ligands affects intermolecular interactions. The nature of the $(B_9C_2H_{11})-M-(B_9C_2H_{11})$ 'sandwich' bond is a matter of discussion. In early studies, this bond was considered as an analogue of the $M-C_5H_5$ π-bond in $M(\pi\text{-}C_5H_5)_2$ metallocenes. This assumption was based on the similarity of the geometric structure of $M-(B_9C_2H_{11})^-$ with the 'sandwich'-type structure formed by the M atom and the cyclopentadienyl anion. Later, the concept regarding the nature of the $M-(B_9C_2H_{11})^{2-}$ bond changed: it is now believed that more considerable σ-bonding (σ-delocalisation) occurs in these complexes in comparison with the interaction of the delocalised π-electronic system of $C_5H_5^-$ with the metal atom in $M(\pi\text{-}C_5H_5)_2$ (see Refs 230 and 246 and references therein). Therefore, dicarbollyl complexes are 'sandwich' cluster systems to a considerable extent. In most cases, charge transfer from the ligand to the metal atom occurs in these compounds.

X-Ray BK_α-emission spectra of dicarbollyl complexes[230] are presented in Fig. 28 along with L_α-spectra of the central atoms. It was shown that an increase in the number of electrons in a metal 3d-shell results in a decrease in the energy band occupied by the HOMOs mainly formed with participation of electrons of that shell. In fact, the half-width of the FeL_α-line is ~6.0 eV, that of CoL_α is ~4.0 eV and that of NiL_α is ~3.0 eV. On the other hand, the binding energy of electrons of this group of orbitals increases in the same order. In fact, the energy of ML_α-lines for metals in dicarbollyl complexes relative to the Fermi level is ~2.5 eV for FeL_α, ~3.2 eV for CoL_α and ~4.2 eV for NiL_α. Thus, metal 3d-AOs make the main contribution to the HOMOs, whereas the MOs composed with participation of the boron 2p-AO lie deeper. Their energy is ~6.5 eV relative to the Fermi level. The strong overlapping of the BK_α- and L_α-bands may be evidence of efficient interaction of ligands with the central metal atom. Transition from the Ni^{III} complex to the Ni^{IV} complex stabilises the MOs composed with involvement of 3d-AOs even more and enhances the B2p–Ni3d interaction. Let us note the high stability of the energy position of the MO with a considerable contribution of the 2p-AO of the boron atom, which is probably caused by the aromatic character of closed three-dimensional systems.

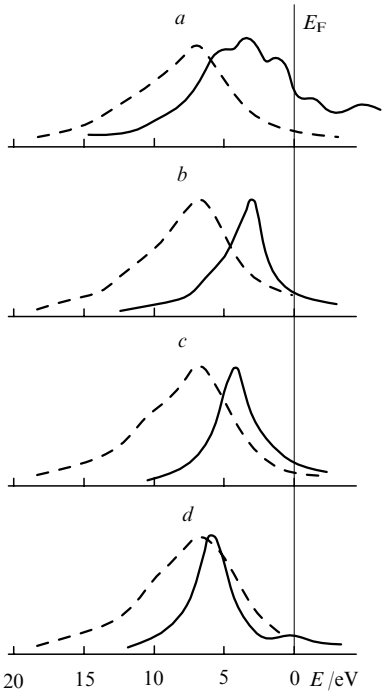


Figure 28. X-Ray BK_α and ML_α emission spectra (dashed and solid lines, respectively) of Cs[(1,2-$B_9C_2H_{11})_2$M] dicarbollyl complexes.[230]
M = Fe (*a*), Co (*b*), Ni (*c*), (1,2-$B_9C_2H_{11})_2$Ni (*d*).

6. Heterocyclic boron compounds

To our knowledge, heterocyclic boron compounds have only been studied by Doering *et al.*[247] They studied the electron energy loss spectra of borazine (point symmetry group D_{3h}) (Fig. 29), which were noted (see Section III.2) to be similar to X-ray absorption spectra. According to the results of these studies, the π-system orbital (e'') is the LUMO in the $B_3N_3H_6$ molecule; it manifests itself as an intense low-energy maximum in the spectra. It should

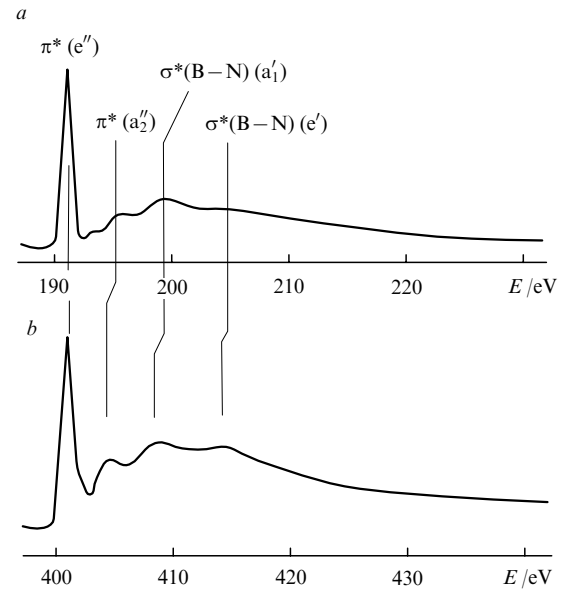


Figure 29. Electron energy loss spectra of borazine.[247]
(*a*) BK spectra; (*b*) NK spectra.

be added that certain details of electronic structures of a number of five- and six-membered boron-containing heterocycles were studied rather thoroughly by UPS and NMR spectroscopies.[83] Figure 7 shows a scheme of interaction of nitrogen and boron AOs and a qualitative scheme of MOs in some heterocyclic boron compounds. These systems involve π-bonding.[83, 87]

V. Conclusion

In this review, it was shown for boron-containing systems as an example that X-ray spectral studies provide vast information about the electronic structures of chemical compounds. A specific feature of X-ray spectroscopy is that it provides information on the energy positions and structures of MOs which is comparable with results of quantum-chemical calculations. Although detailed information about the properties of occupied and vacant orbitals can be extracted from X-ray emission and absorption spectra, it seems most efficient to use these methods in combination with UV and X-ray photoelectron spectra reduced to a common energy scale. The use of absorption spectra, quantum yield spectra and energy loss spectra is especially beneficial for studies of boron compounds that possess acceptor properties. However, because of problems associated with the methods and instruments used, comprehensive X-ray spectral studies with involvement of UPS and XPS have as yet been carried out for a rather limited number of compounds.

A distinctive feature of studies on the electronic structures of chemical compounds of boron is associated with donor–acceptor interactions. In fact, clear detection of a lone electron pair of a donor molecule (HOMO) in X-ray emission spectra and a lone hole pair of an acceptor molecule (LUMO) (with a boron compound as an acceptor) in the absorption spectra, as well as changes in the electronic structures of these molecules upon adduct formation that are observable in X-ray spectra, made this a promising method for studies on the nature of donor–acceptor interaction. Studies of this interaction are based on the two-level model, according to which the formation of a bond only involves the HOMO of the donor and the LUMO of the acceptor; however, this is only an approximate model. The formation of this type of chemical bonds also involves deeper valence MOs of the donor and the acceptor. It is possible that this mechanism can be expanded for the donor–acceptor ligand–metal interaction in complex compounds; the results of its X-ray spectral studies are generalised in the monograph by Mazalov and Yumatov.[241]

This review was written with partial financial support from the Russian Foundation for Basic Research (Project No. 01-03-32428a).

References

1. R B King (Ed.) *Boron Chemistry at the Millennium* (Amsterdam: Elsevier, 1999)
2. *Inorg. Chim. Acta* **289** (1–2) (1999)
3. *J. Organomet. Chem.* **581** (1–2) (1999)
4. E L Muetterties *The Chemistry of Boron and its Compounds* (New York: Wiley, 1967)
5. F N Tavadze, G V Samsonova, G V Tsagareishvili, M E Antadze, N A Zoidze (Eds) *Bor, Poluchenie, Struktura i Svoistva. Materialy IV Mezhdunarodnogo Simpoziuma po Boru* (Boron, Preparation, Structure and Properties. Proceedings of IVth International Symposium on Boron) (Moscow: Nauka, 1974)
6. R D Shannon *Acta Crystallogr. Sect. A* **32** 751 (1976)
7. A V Nikolaev *Fiziko-Khimicheskoe Izuchenie Prirodnykh Boratov* (Physicochemical Investigation of Natural Borates) (Moscow, Leningrad: Izd. Akad. Nauk SSSR, 1947)
8. G V Samsonov, L Ya Markovskii, A F Zhigach, M G Valyashko *Bor. Ego Soedineniya i Splavy* (Boron. Its Compounds and Alloys) (Kiev: Izd. Akad. Nauk Ukr. SSR, 1960)
9. I Ya Nekrasov, A P Grigor'ev, T A Grigor'eva, A A Brovkin, E N Diman, P G Novgorodov, V S Suknev, L V Nikishova *Izuchenie Vysokotemperaturnykh Boratov* (Study of High-Temperature Borates) (Ed. A V Nikolaev) (Moscow: Nauka, 1970)
10. N N Greenwood, in *Comprehensive Inorganic Chemistry* (Ed. A F Trotman-Diskenson) (Oxford: Pergamon Press, 1973) p. 665
11. G K Gode *Boraty Shchelochnozemel'nykh Metallov* (Borates of Alkaline-Earth Metals) (Riga: Zinatne, 1986)
12. A L Ivanovskii, G P Shveikin *Kvantovaya Khimiya v Materialovedenii. Bor, Ego Splavy i Soedineniya* (Quantum Chemistry in the Science of Materials. Boron, Its Alloys and Compounds) (Ekaterinburg: Izd. Ekaterinburg, 1997)
13. D Emin, T L Aselage, A C Switendick, B Morosin, C L Beckel (Eds) *Boron-Rich-Solids. AIP Conference Proceedings* Vol. 231 (New York: American Institute of Physics, 1990)
14. F N Tavadze, I A Bairamashvili, G V Tsagareishvili, K P Tsomaya, N A Zoidze *Kristallografiya* **9** 918 (1964) [a]
15. L V Gurvich, G V Karachevtsev, V N Kondrat'ev, Yu A Lebedev, V A Medvedev, V K Potapov, Yu S Khodeev *Energii Razryva Svyazei. Potentsialy Ionizatsii i Srodstvo k Elektronu* (Energies of Bond Rupture. Ionisation Potential and Electron Affinity) (Ed. V N Kondrat'ev) (Moscow: Nauka, 1974)
16. E B Treivus, Yu O Punin, T V Ushakovskaya, O I Artamonova *Kristallografiya* **20** 199 (1975) [a]
17. L S Palatnik, A A Nechitailo, A A Koz'ma *Dokl. Akad. Nauk SSSR* **261** 1134 (1981) [b]
18. V V Volkov, G S Yur'ev *Izv. Sib. Otd. Akad. Nauk, Ser. Khim. Nauk* **9** (3) 16 (1988)
19. R B Kotel'nikov, S N Bashlakov, Z G Galiakbarova, A I Kashtanov *Osobotugoplavkie Elementy i Soedineniya (Spravochnik)* [Super-Refractory Elements and Compounds (Handbook)] (Moscow: Metallurgiya, 1969)
20. Yu B Kuz'ma *Kristallokhimiya Boridov* (Crystal Chemistry of Borides) (L'vov: Vishcha Shkola, 1983)
21. P S Kislyi, V A Neronov, T A Prikhna, Yu V Bevza *Boridy Alyuminiya* (Aluminium Borides) (Kiev: Naukova Dumka, 1990)
22. G P Shveikin, A L Ivanovskii *Usp. Khim.* **63** 751 (1994) [*Russ. Chem. Rev.* **63** 711 (1994)]
23. R Kiesseling *Acta Chem. Scand.* **4** 209 (1950)
24. T Guo, C M Jin, R E Smalley *J. Phys. Chem.* **95** 4948 (1991)
25. G V Samsonov *Nitridy* (Nitrides) (Kiev: Naukova Dumka, 1969)
26. G V Samsonov, O P Kulik, V S Polishchuk *Poluchenie i Metody Analiza Nitridov* (Production and Methods of Analysis of Nitrides) (Kiev: Naukova Dumka, 1978)
27. G V Samsonov, in *Metallokeramicheskie Materialy i Metody ikh Issledovaniya* (Metal-Ceramic Materials and Methods of Their Investigation) (Kiev: Izd. Akad. Nauk Ukr. SSR, 1959) p. 36
28. A S Bolgar, V F Litvinenko *Termodinamicheskie Svoistva Nitridov* (Thermodynamic Properties of Nitrides) (Kiev: Naukova Dumka, 1980)
29. V S Lysanov (Ed.) *El'bor v mashinostroenii* (Elboron in Mechanical Engineering) (Leningrad: Mashinostroenie, 1978)
30. F Matsui *Tool Eng. Jpn.* **23** 22 (1979)
31. M Matsuo *Newer Metal Ind. Jpn.* **16** 241 (1971)
32. E A Smith *Powder Metall.* **14** 110 (1971)
33. F P Bundy, R H Wentorf Jr *J. Chem. Phys.* **38** 1144 (1963)
34. A V Kurdyumov, A N Pilyankevich *Fazovye Prevrashcheniya v Uglerode i Nitride Bora* (Phase Transformations in Carbon and Boron Nitride) (Kiev: Naukova Dumka, 1979)
35. A V Kurdyumov, A N Pilyankevich, I N Frantsevich *Fiz. Tekhn. Vys. Davl.* (1) 23 (1980)
36. R Taylor, C A Coulson *Proc. Phys. Soc., Sect. A* **65** 834 (1952)
37. E Tegeler, N Kosuch, G Wiech, A Faessler *Phys. Status Solidi B* **91** 223 (1979)
38. Y F Tsay, A Vaidyanathan, S S Mitra *Phys. Rev. B* **19** 5422 (1979)
39. V A Fomichev, T M Zimkina, I I Lyakhovskaya *Fiz. Tv. Tela* **12** 156 (1970) [c]
40. A G Massey *Adv. Inorg. Chem. Radiochem.* **10** 1 (1967)

41. I G Ryss *Khimiya Ftora i Ego Neorganicheskikh Ftoridov* (The Chemistry of Fluorine and Its Inorganic Fluorides) (Moscow: Goskhimizdat, 1956)
42. V I Nefedov, V I Vovna *Elektronnaya Struktura Khimicheskikh Soedinenii* (Electronic Structure of Chemical Compounds) (Moscow: Nauka, 1987)
43. L Åsbrink, A Svenson, W von Niessen, G Bieri *J. Electron. Spectrosc. Relat. Phenom.* **24** 293 (1981)
44. R Manne, K Wittel, B S Mohanty *J. Mol. Phys.* **29** 485 (1975)
45. P L Timms *J. Am. Chem. Soc.* **89** 1629 (1967)
46. K A Solntsev, A M Mebel', N A Votinova, N T Kuznetsov, O P Charkin *Koord. Khim.* **18** 340 (1992) [d]
47. A Stock *Hydrides of Boron and Silicon* (Ithaca, NY: Cornell University Press; London: Oxford University Press, 1933)
48. R M Adams (Ed.) *Boron, Metallo-Boron Compounds and Boranes* (New York: Interscience, 1964)
49. R L Hughes, I C Smith, E W Lawless *Production of the Boranes and Related Research* (New York: Academic Press, 1967)
50. A F Zhigach, D S Stasinevich *Khimiya Gidridov* (The Chemistry of Hydrides) (Leningrad: Khimiya, 1969)
51. E L Muetterties, W H Knoth *Polyhedral Boranes* (New York: Marcel Dekker, 1968)
52. R N Grimes *Carboranes* (New York: Academic Press, 1970)
53. L I Zakharkin, V N Kalinin *Usp. Khim.* **43** 1207 (1974) [*Russ. Chem. Rev.* **43** 551 (1974)]
54. E L Muetterties (Ed.) *Boron Hydride Chemistry* (New York: Academic Press, 1975)
55. M F Hawthorne *J. Organomet. Chem.* **100** 97 (1975)
56. R N Grimes (Ed.) *Metal Interactions with Boron Clusters* (New York: Plenum, 1982)
57. F I Yanovskii *Usp. Khim.* **54** 881 (1985) [*Russ. Chem. Rev.* **54** 515 (1985)]
58. R E Williams *Chem. Rev.* **92** 177 (1992)
59. N N Greenwood *Chem. Soc. Rev.* **21** 49 (1992)
60. P J Fazen, E E Remsen, J S Beck, P J Carroll, A R McGhie, L G Sneddon *Chem. Mater.* **7** 1942 (1995)
61. R N Grimes *Appl. Organomet. Chem.* **10** 209 (1996)
62. J Bould, W Clegg, S J Teat, L Barton, N P Rath, M Thornton-Pett, J D Kennedy *Inorg. Chim. Acta* **289** 95 (1999)
63. N S Hosmane *J. Organomet. Chem.* **581** 13 (1999)
64. H C Longuet-Higgins *Quart. Rev.* **11** 121 (1957)
65. W N Lipscomb *Boron Hydrides* (New York: Benjamin, 1963)
66. W N Lipscomb *Pure Appl. Chem.* **49** 701 (1977)
67. W N Lipscomb, in *Boron Chemistry-4* (Eds R W Parry, G Kodama) (Oxford: Pergamon Press, 1980) p. 1
68. K Wade *Adv. Inorg. Chem. Radiochem.* **18** 1 (1976)
69. R E Williams *Adv. Inorg. Chem. Radiochem.* **18** 67 (1976)
70. K Wade, in *Boron Chemistry-4* (Eds R W Parry, G Kodama) (Oxford: Pergamon Press, 1980) p. 23
71. R Hoffmann, W N Lipscomb *J. Chem. Phys.* **36** 3489 (1962)
72. J Aihara *J. Am. Chem. Soc.* **100** 3339 (1978)
73. B W Clare, D L Kepert *Inorg. Chem.* **23** 1521 (1984)
74. R B King *Izv. Akad. Nauk, Ser. Khim.* 1353 (1993) [e]
75. P von R Schleyer, H Jiao, K Najafian, G Subramanian, M Hofmann, in *The Ninth International Meeting on Boron Chemistry* (*Program and Abstracts*) (Heidelberg: Ruprecht-Karls-Universität, 1996) p. 13
76. R J Wiersema, M F Hawthorne *J. Am. Chem. Soc.* **96** 761 (1974)
77. J H Hall, D A Dixon, D A Kleier, T A Halgren, L D Brown, W N Lipscomb *J. Am. Chem. Soc.* **97** 4202 (1975)
78. V V Volkov, V N Ikorskii *Izv. Sib. Otd. Akad. Nauk SSSR, Ser. Khim. Nauk* **14** (6) 38 (1981)
79. V V Volkov, V N Ikorskii, S T Dunaev *Izv. Akad. Nauk SSSR, Ser. Khim.* 973 (1988) [e]
80. N N Greenwood, I M Ward *Chem. Soc. Rev.* **3** 231 (1974)
81. A Stock, E Pohland *Chem. Ber.* **59** 2215 (1926)
82. E Wiberg *Naturwissenschaften* **35** 212 (1948)
83. D Nölle, H Nöth *Z. Naturforsch., B* **27** 1425 (1972)
84. V V Korshak, V A Zamyatina, N I Bekasova *Bororganicheskie Polimery* (Organoboron Polymers) (Moscow: Nauka, 1975)
85. B M Mikhailov *Pure Appl. Chem.* **49** 749 (1977)
86. W Siebert, in *Boron Chemistry-4* (Eds R W Parry, G Kodama) (Oxford: Pergamon Press, 1980) p. 81
87. H Nöth, in *Boron Chemistry-4* (Eds R W Parry, G Kodama) (Oxford: Pergamon Press, 1980) p. 109
88. R N Grimes *Chem. Rev.* **92** 251 (1992)
89. A N Nesmeyanov, R A Sokolik *Metody Elementoorganicheskoi Khimii. Bor, Alyuminii, Gallii, Indii, Tallii* (The Methods of Organoelement Chemistry. Boron, Aluminium, Gallium, Indium, Thallium) (Moscow: Nauka, 1964)
90. B M Mikhailov, Yu N Bubnov *Bororganicheskie Soedineniya v Organicheskom Sinteze* (Organoboron Compounds in Organic Synthesis) (Moscow: Nauka, 1977)
91. M A Blokhin *Metody Rentgenospektral'nykh Issledovanii* (The Methods of X-Ray Investigation) (Moscow: Fizmatgiz, 1956)
92. K Siegbahn, C Nordling, A Fahlman, R Nordberg, K Hamrin, J Hedman, G Johansson, T Bergmark, S-E Karlsson, I Lindgren, B Lindberg *ESCA. Atomic, Molecular and Solid State Structure Studied by Means of Electron Spectroscopy, Uppsala* Vol. 20, 1967
93. W L Baun, D W Fisher, in *Spectroscopy in Inorganic Chemistry* Vol. 1 (Eds C N R Rao, J R Ferraro) (New York: Academic Press, 1970) p. 209
94. R L DeKock, D R Lloyd *Adv. Inorg. Chem. Radiochem.* **16** 65 (1974)
95. L N Mazalov, A P Sadovskii, G N Dolenko, E S Gluskin, V D Yumatov, V V Murakhtanov, F Kh Gel'mukhanov, in *Fundamental'nye Issledovaniya. Khimicheskie Nauki* (Fundamental Research. Chemical Sciences) (Novosibirsk: Nauka, 1977) p. 77
96. L N Mazalov, V D Yumatov, V V Murakhtanov, F Kh Gel'mukhanov, G N Dolenko, E S Gluskin, A V Kondratenko *Rentgenovskie Spektry Molekul* (X-Ray Spectra of Molecules) (Novosibirsk: Nauka, 1977)
97. S P Cramer, K O Hodgson *Prog. Inorg. Chem.* **25** 1 (1979)
98. A H Cowley *Prog. Inorg. Chem.* **26** 45 (1979)
99. A Meisel, G Leonhardt, R Szargan *Röntgenspektren und Chemische Binding* (Leipzig: Akademie-Verlag, 1977)
100. V I Nefedov *Rentgenoelektronnaya Spektroskopiya Khimicheskikh Soedinenii* (X-Ray Electron Spectroscopy of Chemical Compounds) (Moscow: Khimiya, 1984)
101. L N Mazalov *Rentgenovskie Spektry i Khimicheskaya Svyaz'* (X-Ray Spectra and Chemical Bond) (Novosibirsk: Nauka, 1982)
102. V I Vovna *Elektronnaya Struktura Organicheskikh Soedinenii* (Electronic Structure of Organic Compounds) (Moscow: Nauka, 1991)
103. Yu A Teterin, S G Gagarin *Usp. Khim.* **65** 895 (1996) [*Russ. Chem. Rev.* **65** 825 (1996)]
104. T M Zimkina, V A Fomichev *Ul'tramyagkaya Rentgenovskaya Spektroskopiya* (Ultrasoft X-Ray Spectroscopy) (Leningrad: Leningrad State University, 1971)
105. G N Kulipanov, A N Skrinskii *Usp. Fiz. Nauk* **122** 369 (1977) [f]
106. C Kunz (Ed.) *Synchrotron Radiation. Techniques and Applications* (Berlin: Springer, 1979)
107. I M Ternov, V V Mikhailin *Sinkhrotronnoe Izluchenie. Teoriya i Eksperiment* (Synchrotron Radiation. Theory and Experiment) (Moscow: Energoatomizdat, 1986)
108. G R Wight, C E Brion, M J Van Der Wiel *J. Electron Spectrosc. Relat. Phenom.* **1** 457 (1972/73)
109. C E Brion, S Daviel, R Sodhi, A P Hitchcock, in *X-Ray Atomic Inner-Shell Physics (AIP Conference Proceedings)* (New York: American Institute of Physics, 1982) Vol. 94, p. 429
110. E N Gur'yanova, I P Gol'dshtein, I M Romm *Donorno-Aktseptornaya Svyaz'* (Donor – Acceptor Bond) (Moscow: Khimiya, 1973)
111. O Kh Poleshchuk, Yu K Maksyutin *Usp. Khim.* **45** 2097 (1976) [*Russ. Chem. Rev.* **45** 1077 (1976)]
112. I M Romm, E N Gur'yanova *Usp. Khim.* **55** 225 (1986) [*Russ. Chem. Rev.* **55** 83 (1986)]
113. R C Ehlert, R A Mattson *Adv. X-Ray Anal.* **9** 456 (1965)
114. D W Fischer, W L Baun *J. Appl. Phys.* **37** 768 (1966)
115. V A Fomichev *Fiz. Tv. Tela* **9** 3167 (1967) [c]
116. Y Hayasi *Sci. Rep. Tôhoku Univ., Ser. 1* **51** (3) 43 (1968)
117. E P Domashevskaya, N E Solovjev, V A Terekhov, Ya A Ugai *J. Less-Common. Met.* **47** 189 (1976)
118. S Luck, D S Urch *Phys. Scr.* **41** 749 (1990)

119. Ph McClusky, D S Urch *Phys. Scr.* **41** 878 (1990)
120. S Luck, D S Urch *Phys. Scr.* **41** 970 (1990)
121. W L O'Brien, J Jia, Q-Y Dong, T A Callcott, K E Miyano, D L Ederer, D R Mueller, C-C Kao *Phys. Rev. Lett.* **70** 238 (1993)
122. Y Muramatsu, M Oshima, J Kawai, H Kato *Nucl. Instrum. Methods Phys. Res., Sect. B* **75** 559 (1993)
123. Y Muramatsu, M Oshima, H Kato *Phys. Rev. Lett.* **71** 448 (1993)
124. Y Muramatsu, J Kawai, T Scimeca, M Oshima, H Kato *Phys. Scr.* **50** 25 (1994)
125. M Yanagihara, N Miyata, M Furudate, T Ejima, M Watanabe *J. Electron Spectrosc. Relat. Phenom.* **79** 187 (1996)
126. E Z Kurmaev, A V Ezhov, S N Shamin, V M Cherkashenko, Yu G Andreev, T Lundstrlm *J. Alloys Compd.* **248** 86 (1997)
127. Y Muramatsu, H Takenaka, T Oyama, T Hayashi, M M Grush, R C C Perera *X-Ray Spectrom.* **28** 503 (1999)
128. K-H Hallmeier, R Szargan, A Meisel, E Hartmann, E S Gluskin *Spectrochim. Acta, Part A* **37** 1049 (1981)
129. E J Esposto, P Aebi, T Tyliszczak, A P Hitchcock, M Kasrai, J D Bozek, T E Jackman, S R Rolfe *J. Vac. Sci. Technol. A* **9** 1663 (1991)
130. D Li, G M Bancroft, M E Fleet *J. Electron Spectrosc. Relat. Phenom.* **79** 71 (1996)
131. R Franke, S Bender, J Hormes, A A Pavlychev, N G Fominych *Chem. Phys.* **216** 243 (1997)
132. B Gilbert, L Perfetti, O Fauchoux, J Redondo, P-A Baudat, R Andres, M Neumann, S Steen, D Gabel, D Mercanti, M T Ciotti, P Perfetti, G Margaritondo, G De Stasio *Phys. Rev. E* **62** 1110 (2000)
133. D J Joyner, D M Hercules *J. Chem. Phys.* **72** 1095 (1980)
134. M S Nakhmanson, V I Baranovskii *Fiz. Tv. Tela* **12** 2458 (1970) [c]
135. J Kawai, K Maeda, I Higashi, M Takami, Y Hayasi, M Uda *Phys. Rev. B* **42** 5693 (1990)
136. J Kawai *Adv. Quantum Chem.* **29** 329 (1997)
137. J Kawai, Y Muramatsu, A Agui, S Shin, H Kato *Spectrochim. Acta, Part B* **52** 593 (1997)
138. A P Sadovskii, L I Nasonova *Zh. Strukt. Khim.* **18** 673 (1977) [g]
139. S V Nekipelov, V N Akimov, A S Vinogradov *Fiz. Tv. Tela* **33** 663 (1991) [c]
140. V A Fomichev *Izv. Akad. Nauk SSSR, Ser. Fiz.* **31** 957 (1967)
141. O Aita, T Sagawa *J. Phys. Soc. Jpn.* **27** 164 (1969)
142. L Hoffmann, G Wiech, E Zöpf *Z. Phys.* **229** 131 (1969)
143. I I Lyakhovskaya, T M Zimkina, V A Fomichev *Izv. Akad. Nauk SSSR, Ser. Fiz.* **36** 393 (1972)
144. E Sobczak, K Persy *Phys. Scr.* **22** 88 (1980)
145. M Kawaguchi, Y Wakukawa, H Nakamura *J. Phys. Chem. B* **104** 5869 (2000)
146. E A Zhurakovskii *Elektronnaya Struktura Tugoplavkikh Soedinenii* (ElectronicStructure of Refractory Compounds) (Kiev: Naukova Dumka, 1976)
147. J Nagamatsu, N Nakagawa, T Muranaka, Y Zenitani, J Akimitsu *Nature (London)* **410** 63 (2001)
148. A L Ivanovskii *Usp. Khim.* **70** 811 (2001) [*Russ. Chem. Rev.* **70** 717 (2001)]
149. I Jiménez, D G J Sutherland, T van Buuren, J A Carlisle, L J Terminello, F J Himpsel *Phys. Rev. B* **57** 13167 (1998)
150. I Jiménez, L J Terminello, F J Himpsel, M Grush, T A Callcot *J. Electron Spectrosc. Relat. Phenom.* **101 – 103** 611 (1999)
151. M A Rumsh, V A Fomichev, T M Zimkina, I I Zhukova *Vestn. Leningr. Univ., Fiz. Khim.* **16** (3) 49 (1968)
152. V A Fomichev, M A Rumsh *J. Phys. Chem. Solids* **29** 1015 (1968)
153. V A Fomichev *Fiz. Tv. Tela* **13** 907 (1971) [c]
154. I N Frantsevich, E A Zhurakovskii, A V Kurdyumov, N N Vasilenko *Dokl. Akad. Nauk SSSR* **203** 87 (1972) [b]
155. H Kohzuki, M Motoyama, T Kaneyoshi, Y Kowada, J Kawai, H Adachi *Surf. Rev. Lett.* **3** 1051 (1996)
156. A S Vinogradov, S V Nekipelov, A A Pavlychev *Fiz. Tv. Tela* **33** 896 (1991) [c]
157. P Widmayer, H-G Boyen, P Ziemann, P Reinke, P Oelhafen *Phys. Rev. B* **59** 5233 (1999)
158. J Barth, C Kunz, T M Zimkina *Solid State Commun.* **36** 453 (1980)
159. Y Muramatsu, M Oshima, J Kawai, S Tadokoro, H Adachi, A Agui, S Shin, H Kato, H Kohzuki, M Motoyama *Phys. Rev. Lett.* **76** 3846 (1996)
160. Y Muramatsu, H Kouzuki, T Kaneyoshi, M Motoyama, A Agui, S Shin, H Kato, J Kawai *Appl. Phys. A: Mater. Sci. Process.* **65** 191 (1997)
161. J J Jia, T A Callcott, E L Shirley, J A Carlisle, L J Terminello, A Asfaw, D L Ederer, F J Himpsel, R C C Perera *Phys. Rev. Lett.* **76** 4054 (1996)
162. A Agui, S Shin, M Fujisawa, Y Tezuka, T Ishii, O Mishima, K Era, E Shigemasa, A Yagishita *J. Electron Spectrosc. Relat. Phenom.* **79** 191 (1996)
163. A Agui, S Shin, M Fujisawa, Y Tezuka, T Ishii, Y Muramatsu, O Mishima, K Era *Phys. Rev. B* **55** 2073 (1997)
164. S Shin, A Agui, Y Harada *J. Synchrotron Radiat.* **4** 256 (1997)
165. K-i Noba, Y Kayanuma, M Yanagihara *J. Phys. Soc. Jpn.* **67** 664 (1998)
166. K Lawniczak-Jablonska, T Suski, I Gorczyca, N E Christensen, K E Attenkofer, R C C Perera, E M Gullikson, J H Underwood, D L Ederer, Z L Weber *Phys. Rev. B* **61** 16623 (2000)
167. A Chaiken, L J Terminello, J Wong, G L Doll, C A Taylor II *Appl. Phys. Lett.* **63** 2112 (1993)
168. D H Berns, M A Cappelli, D K Shuh *Diamond Relat. Mater.* **6** 1883 (1997)
169. I Jiménez, A F Jankowski, L J Terminello, D G J Sutherland, J A Carlisle, G L Doll, W M Tong, D K Shuh, F J Himpsel *Phys. Rev. B* **55** 12025 (1997)
170. A A Pavlychev, R Franke, S Bender, J Hormes *J. Phys.: Condens. Matter* **10** 2181 (1998)
171. P N Semochkin, I B Borovskii *Fiz. Met. Metalloved.* **39** 497 (1975)
172. I B Borovskii, P N Semochkin, M Rzaeva *Fiz. Met. Metalloved.* **39** 537 (1975)
173. C Beyreuther, R Hierl, G Wiech *Ber. Bunsen-Ges. Phys. Chem.* **79** 1081 (1975)
174. A Mansour, S E Schnatterly *Phys. Rev. B* **36** 9234 (1987)
175. E Tegeler, N Kosuch, G Wiech, A Faessler *Phys. Status Solidi B* **84** 561 (1977)
176. M Yanagihara, N Miyata, T Ejima, M Watanabe, Y Kayanuma *J. Phys. Soc. Jpn.* **66** 1626 (1997)
177. F C Brown, R Z Bachrach, M Skibowski *Phys. Rev. B* **13** 2633 (1976)
178. D M Davies, F Bassani, F C Brown, C G Olson *Phys. Rev. B* **24** 3537 (1981)
179. H Shimada, N Matsubayashi, M Imamura, T Sato, Y Kakudate, S Fujiwara, A Nishijima *J. Electron Spectrosc. Relat. Phenom.* **79** 211 (1996)
180. J Moscovici, G Loupias, P Parent, G Tourillon *J. Phys. Chem. Solids* **57** 1159 (1996)
181. R D Leapman, J Silcox *Phys. Rev. Lett.* **42** 1361 (1979)
182. R D Leapman, P L Fejes, J Silcox *Phys. Rev. B* **28** 2361 (1984)
183. E O Filatova, T A Blagoveshchenskaya, S K Kozhakhmetov *Fiz. Tv. Tela* **32** 1551 (1990) [c]
184. E Filatova, A Stepanov, C Blessing, J Friederich, R Barchewitz, J-M André, F Le Guera, S Bac, P Troussel *J. Phys.: Condens. Matter* **7** 2731 (1995)
185. V I Nefedov *Stroenie Molekul i Khimicheskaya Svyaz' (Itogi Nauki i Tekhniki)* [Structure of Molecules and Chemical Bond (Advances of Sciences and Engineering Series)] (Moscow: Izd. VINITI, 1975) Vol. 3
186. V V Ilyasov, N Yu Safontseva, I Ya Nikiforov *Fiz. Tv. Tela* **36** 451 (1994) [c]
187. T P Zhdanova, V V Ilyasov, I Ya Nikiforov *Zh. Struk. Khim.* **39** 1083 (1998) [g]
188. T P Zhdanova, V V Ilyasov, I Ya Nikiforov *Zh. Struk. Khim.* **41** 1149 (2000) [g]
189. A L Ankudinov, B Ravel, J J Rehr, S D Conradson *Phys. Rev. B* **58** 7565 (1998)

190. H Kohzuki, T Kaneyoshi, M Motoyama, Y Kowada, Y Muramatsu, J Kawai, F Kanamaru *Physica B* **229** 306 (1997)
doi> 191. H Ma, S H Lin, R W Carpenter, P Rice, O F Sankey *J. Appl. Phys.* **73** 7422 (1993)
doi> 192. I Tanaka, H Araki, M Yoshiya, T Mizoguchi, K Ogasawara, H Adachi. *Phys. Rev. B* **60** 4944 (1999)
193. K Hamrin, G Johansson, U Gelius, C Nordling, K Siegbahn *Phys. Scr.* **1** 277 (1970)
194. V G Aleshin, A N Sokolov, A A Shul'zhenko *Sverkhtv. Mater.* **5** 12 (1985)
doi> 195. V A Fomichev, I I Zhukova, I K Polushina *J. Phys. Chem. Solids* **29** 1025 (1968)
196. V A Fomichev *Fiz. Tv. Tela* **15** 1286 (1973) [c]
197. A Agui, S Shin, Y Kumashiro *J. Phys. Soc. Jpn.* **68** 166 (1999)
198. V V Nemoshkolenko, V G Aleshin *Fiz. Tv. Tela* **12** 59 (1970) [c]
199. V D Yumatov, V V Murakhtanov, V V Volkov, O L Shcheka, E A Il'inchik, G G Furin *Zh. Neorg. Khim.* **40** 131 (1995) [h]
200. V A Fomichev, R L Barinskii *Zh. Strukt. Khim.* **11** 875 (1970) [g]
201. W Hayes, F C Brown *J. Phys. B* **4** L85 (1971)
doi> 202. E Ishiguro, S Iwata, Y Suzuki, A Mikuni, T Sasaki *J. Phys. B, At. Mol. Phys.* **15** 1841 (1982)
doi> 203. H Kanamori, S Iwata, A Mikuni, T Sasaki *J. Phys. B, At. Mol. Phys.* **17** 3887 (1984)
204. T M Zimkina, A S Vinogradov *Izv. Akad. Nauk SSSR, Ser. Fiz.* **36** 248 (1972)
205. S V Nekipelov, V N Akimov, A S Vinogradov *Opt. Spektrosk.* **64** 817 (1988) [i]
doi> 206. Y Shimizu, K Ueda, H Chiba, M Okunishi, J B West, Y Sato, T Hayashi *J. Chem. Phys.* **107** 2419 (1997)
207. R Camilloni, E Fainelli, G Petrocelli, G Stefani, F Maracci, R Platania *Lect. Notes Chem.* **35** 172 (1984)
doi> 208. M Tronc, L Malegat, R Azria, Y Le Coat *J. Phys. B, At. Mol. Phys.* **15** L253 (1982)
209. J L Dehmer *J. Chem. Phys.* **56** 4496 (1972)
doi> 210. M B Robin *Chem. Phys. Lett.* **31** 140 (1975)
211. W H E Schwarz, L Mensching, K H Hallmeier, R Szargan *Chem. Phys.* **82** 57 (1983)
doi> 212. F Sette, J Stöhr, A Hitchcock *J. Chem. Phys.* **81** 4906 (1984)
doi> 213. N Kosugi, T Yokoyama, H Kuroda *Chem. Phys.*, **104** 449 (1986)
214. S V Nekipelov, V N Akimov, A S Vinogradov *Fiz. Tv. Tela* **30** 3647 (1988) [c]
215. A A Pavlychev, A S Vinogradov, V N Akimov, S V Nekipelov *Phys. Scr.* **41** 160 (1990)
doi> 216. K Ueda, K Ohmori, M Okunishi, H Chiba, Y Shimizu, Y Sato, T Hayaishi, E Shigemasa, A Yagishita *Phys. Rev. A* **52** R1815 (1995)
217. K Ueda *J. Electron Spectrosc. Relat. Phenom.* **88–91** 1 (1998)
doi> 218. G Hagenow, W Denzer, H-W Jochims, H Baumgirtel *Chem. Phys. Lett.* **195** 267 (1992)
219. M S Nakhmanson, V I Baranovskii *Teor. Eksp. Khim.* **7** 15 (1971) [j]
doi> 220. J R Swanson, Dan Dill, J L Dehmer *J. Chem. Phys.* **75** 619 (1981)
221. F A Gianturco, E Semprini, F Stefani *Il Nuovo Cimento D* **2** 687 (1983)
doi> 222. S Tanaka, Y Kayanuma, K Ueda *Phys. Rev. A* **57** 3437 (1998)
223. P J Bassett, D R Lloyd *J. Chem. Soc., Chem. Commun.* 36 (1970)
224. W L Jolly, K D Bomben, C J Eyermann *At. Data Nucl. Data Tables* **31** 433 (1984)
doi> 225. K Ueda, H Chiba, Y Sato, T Hayaishi, E Shigemasa, A Yagishita *J. Chem. Phys.* **101** 7320 (1994)
doi> 226. K Ueda, S Tanaka, Y Shimizu, Y Muramatsu, H Chiba, T Hayashi, M Kitajima, H Tanaka *Phys. Rev. Lett.* **85** 3129 (2000)
227. K Kimura, S Katsumata, Y Achiba, T Yamazaki, S Iwata *Handbook of HeI Photoelectron Spectra of Fundamental Organic Molecules* (Tokyo: Japan Scientific Societies Press, New York: Halsted Press, 1981)
228. V N Akimov, A S Vinogradov, A V Zhadenov *Opt. Spektrosk.* **65** 349 (1988) [i]
229. V D Yumatov, V V Murakhtanov, N F Salakhutdinov, A V Okotrub, L N Mazalov, L G Logunova, V A Koptyug, G G Furin *Zh. Strukt. Khim.* **28** (5) 73 (1987) [g]
230. E A Il'inchik, V V Volkov, K G Myakishev, V D Yumatov, I P Asanov, G F Khudorozhko, O L Shcheka, L N Mazalov, in *Khimiya Neorganicheskikh Gidridov* (The Chemistry of Inorganic Hydrides) (Ed. N T Kuznetsov) (Moscow: Nauka, 1990) p. 67
231. J Arber, D S Urch, in *International Conference on X-Ray and Inner-Shell Processes in Atoms, Molecules and Solids (Abstracts of Reports), Leipzig, 1984* Pt. 1, p. 17
232. O L Shcheka, V D Yumatov, G G Furin *Zh. Fiz. Khim.* **70** 278 (1996) [k]
233. V V Volkov, E A Il'inchik, L N Mazalov, V D Yumatov, G F Khudorozhko *Izv. Akad. Nauk SSSR, Ser. Khim.* 1640 (1982) [e]
doi> 234. A V Okotrub, L G Bulusheva, V V Volkov *J. Mol. Struct.* **520** 33 (2000)
235. A P Hitchcock, A T Wen, S W Lee, J A Glass Jr, J T Spenser, P A Dowben *J. Phys. Chem.* **97** 8171 (1993)
doi> 236. S Lee, P A Dowben, A T Wen, A P Hitchcock, J A Glass Jr, J T Spenser *J. Vac. Sci. Technol., A* **10** 881 (1992)
237. V V Volkov, E A Il'inchik, G F Khudorozhko, V D Yumatov, L N Mazalov *Izv. Akad. Nauk SSSR, Ser. Khim.* 2248 (1985) [e]
238. V D Yumatov, E A Il'inchik, V V Murakhtanov, S T Dunaev, V V Volkov *Zh. Neorg. Khim.* **38** 423 (1993) [h]
239. V V Murakhtanov, T M Polyanskaya, V V Volkov *Zh. Strukt. Khim.* **37** 652 (1996) [g]
240. V D Yumatov, V V Murakhtanov, V V Volkov, E A Il'inchik, O V Volkov *Zh. Neorg. Khim.* **43** 1677 (1998) [h]
241. L N Mazalov, V D Yumatov *Elektronnoe Stroenie Ekstragentov* (Electronic Structures of Extractants) (Novosibirsk: Nauka, 1984)
242. V D Yumatov, E A Il'inchik, V V Murakhtanov, V V Volkov, L N Mazalov, in *The XXIXth Colloquium. Spectroscopicum Internationale (Book of Abstracts), Leipzig, 1995* p. 409
243. E A Il'inchik, V V Volkov, O V Volkov, S T Dunaev, G S Voronina *Sravnitel'noe Issledovanie Elektronnogo Stroeniya Boranovykh i Tiaboranovykh Kompleksov. Preprint 90-05* (Comparative Investigation of Electronic Structures of Borane and Thiaborane Complexes. Preprint 90-05) (Novosibirsk: Institute of Inorganic Chemistry, Siberian Branch of Academy of Sciences of the USSR, 1990)
244. E A Il'inchik, V V Volkov, O V Volkov *Zh. Strukt. Khim.* **40** 358 (1999) [g]
245. V D Yumatov, E A Il'inchik, L N Mazalov, O V Volkov, V V Volkov *Zh. Strukt. Khim.* **42** 338 (2001) [g]
246. L N Mazalov, V V Volkov, S Ya Dvurechenskaya, L I Nasonova *Zh. Neorg. Khim.* **23** 1860 (1978) [h]
247. J P Doering, A Gedanken, A P Hitchcock, P Fischer, J Moore, J K Olthoff, J Tossell, K Raghavachari, M B Robin *J. Am. Chem. Soc.* **108** 3602 (1986)

[a] — *Crystallogr. Rep. (Engl. Transl.)*
[b] — *Dokl. Chem. (Engl. Transl.)*
[c] — *Phys. Solid State (Engl. Transl.)*
[d] — *Russ. J. Coord. Chem. (Engl. Transl.)*
[e] — *Russ. Chem. Bull., Int. Ed. (Engl. Transl.)*
[f] — *Physics-Uspekhi (Engl. Transl.)*
[g] — *J. Struct. Chem. (Engl. Transl.)*
[h] — *Russ. J. Inorg. Chem. (Engl. Transl.)*
[i] — *Opt. Spectrosc. (Engl. Transl.)*
[j] — *Theor. Exp. Chem. (Engl. Transl.)*
[k] — *Russ. J. Phys. Chem. (Engl. Transl.)*